Flow characteristics of a two-phase mixture in an axial spool valve

by

George Rexford Schade

A Dissertation Submitted to the
Graduate Faculty in Partial Fulfillment of
The Requirements for the Degree of
DOCTOR OF PHILOSOPHY

Majors: Mechanical Engineering
Electrical Engineering

Approved:

Signature was redacted for privacy.

In Charge of Major Work

Signature was redacted for privacy.

For the Major Departments

Signature was redacted for privacy.

For the Graduate College

Iowa State University
Ames, Iowa

1974

TABLE OF CONTENTS

LIST OF FIGURES

LIST OF TABLES

NOMENCLATURE

Symbol	Units	Description
a	dimensionless	Rate of change of quality as a function of pressure ratio
A	$in.^2$	Orifice area
$b_i, i=1,4$	dimensionless	Coefficients of incompressible flow discharge coefficient function of flow number
C	dimensionless	Discharge coefficient
C_r	in.	Spool radial clearance
D	in.	Spool valve diameter
G	$lb.sec./in.^3$	Mass velocity of fluid in duct
K	dimensionless	Loss coefficient of flow through a sudden contraction in duct area
l	in.	Valve characteristic dimension
M	$in.^2$	Constant
$\dot{m}$	lb.sec./in.	Mass rate of flow
P_1	$lb./in.^2$	Pressure upstream of orifice
P_2	$lb./in.^2$	Pressure downstream of orifice
P_{2t}	$lb./in.^2$	Pressure downstream of orifice at transition from incompressible to compressible flow
ΔP_c	$lb./in.^2$	Pressure drop across a sudden contraction in flow duct area

Q	$in.^3/sec.$	Fluid volume flow rate through orifice
Q_ℓ	$in.^3/sec.$	Liquid phase volume flow rate
Q_1	$in.^3/sec.$	Fluid leakage flow rate through upstream radial clearance gap
Q_2	$in.^3/sec.$	Fluid leakage flow rate through downstream radial clearance gap
R	$in.^2/sec.^2{}^\circ R$	Ideal gas constant for air
T	degrees Rankine	Fluid temperature
v	$in.^4/lb.sec.^2$	Specific volume of fluid
v_f	$in.^4/lb.sec.^2$	Specific volume of liquid
v_g	$in.^4/lb.sec.^2$	Specific volume of gas
v_{fg}	$in.^4/lb.sec.^2$	Difference between the specific volume of the liquid phase and the specific volume of the gas phase
V	in./sec.	Average fluid velocity through orifice
x	dimensionless	Quality of fluid
x_0	dimensionless	Quality of fluid at zero pressure ratio
X_0	in.	Micrometer reading when X=0
X	in.	Spool valve displacement measured from line-on-line position
α	dimensionless	Rate of change of a as a function of flow number

β	dimensionless	Rate of change of x_0 as a function of flow number
δ	dimensionless	Increment in discharge coefficient at transition from incompressible to compressible flow
κ	dimensionless	Cavitation number
κ_i	dimensionless	Cavitation number at incipient cavitation
κ_t	dimensionless	Cavitation number at transition from compressible flow to incompressible flow
λ	dimensionless	Flow number
λ_0	dimensionless	Constant
ξ	dimensionless	Pressure factor for evaluating v_{fg}
ν	in.^{2}/sec.	Kinematic viscosity
ρ	lb.sec.^{2}/in.^{4}	Fluid density
ρ_f	lb.sec.^{2}/in.^{4}	Liquid phase density
ψ	dimensionless	Two-phase correction factor

INTRODUCTION

In order to analytically synthesize an automatic control system, it is necessary to be able to predict the performance and stability of the system. This, in turn, requires knowledge of the performance characteristics of each of the important elements of the system, preferably expressed in the form of mathematical functions. One important element of many hydraulic systems is the spool valve (figure 1), which is used as a throttling device to control fluid flow rates. The relationship between valve opening, flow rate through the opening, and pressure upstream and downstream of the valve must be known in order to determine the proper size of the valve in relation to other elements in the system. This relationship directly affects the performance and stability of the overall system.

There are several factors known to affect the flow through an axial spool valve. Geometry of the valve is obviously important. In a spool valve with no clearance between spool and valve body, the orifice area is proportional to valve opening. The flow is complicated by the staggering of the sharp edges that constitute the orifice, in that the edges are misaligned by an amount proportional to valve opening. The situation is further complicated in real valves by the necessity for clearance between spool and valve body. Because of this clearance, flow cannot be cut off completely,

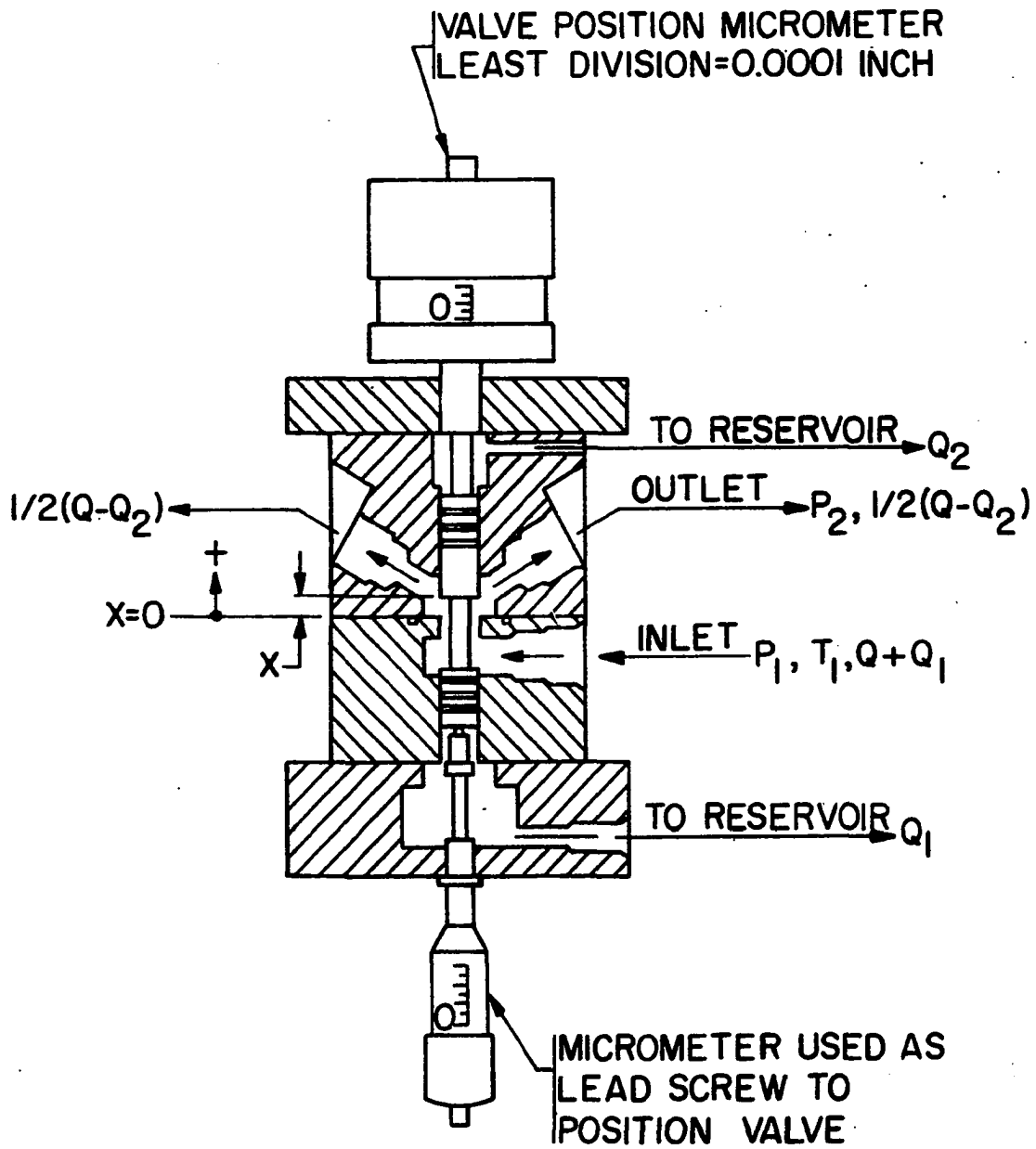

Figure 1. Diagram of test valve

and there will be leakage around the ends of the spool (figure 1, Q_1 and Q_2). If the valve is properly designed, the leakage can have the beneficial effect of hydrostatically lubricating the valve, preventing sticking of the spool in the valve body. But the radial clearance complicates system design because the orifice area is not proportional to axial valve opening.

In an effort to facilitate the design of hydraulic control systems, Donald R. Storjohann proposed a model to predict effective flow area as a function of spool radial clearance and spool position in the valve body (17). He constructed an experimental valve, and conducted a series of tests. Results of his tests confirmed his proposed area model, but revealed other fluid pressure related anomalous spool valve behavior.

Spool Valve Orifice Flow

If a fluid is incompressible, its flow in a sharp edged spool valve orifice should be described by the hydraulic equation:

$$Q = CA\sqrt{\frac{2(P_1-P_2)}{\rho_f}}$$

where:

Q=flow rate

C=orifice flow coefficient

A=flow area

P_1=pressure upstream of orifice

P_2=pressure downstream of orifice, assumed to be the same value as the pressure at the flow vena contracta

ρ_f=density of incompressible liquid

The common practice in spool valve design is to assume that the orifice flow coefficient is constant, a characteristic of the valve. However, Storjohann's tests revealed that for a given valve opening there was considerable variation in C for various P_1 and P_2. Similar results may be seen in the results of tests by Shearer on a 4-way spool valve (16).

For one fixed valve opening, Storjohann tried two schemes of variation in P_1 and P_2--first holding P_1 constant while varying P_2 (to simulate a hydraulic system with a constant supply pressure and varying load pressure), and then holding P_2 constant while varying P_1. There seemed to be less variation in C in the second case, holding P_2 constant while varying P_1. The tests were quite repeatable in both cases.

Later analysis of Storjohann's data by the author showed that the variation in C was a consistent increasing function of the pressure ratio P_2/P_1, both for tests with upstream pressure held constant and with downstream pressure held constant. For the case of P_1 held constant, C was a generally

increasing function of pressure ratio, rising linearly at low pressure ratio, remaining relatively constant at intermediate pressure ratio, and increasing rapidly with increasing slope at high pressure ratio. Results are shown in figure 2.

When plotted as a function of pressure ratio, results for the case of downstream pressure held constant very nearly coincided with the results for the case of upstream pressure held constant. Less variation in C was encountered when downstream pressure was held constant simply because for the same test values of pressure drop across the valve, there was less variation in pressure ratio when downstream pressure was maintained constant. The consistency of the variation of C as a function of pressure ratio implicated fluid compressibility as a cause of the variation, at least for the low pressure ratio test points. It is believed that this compressibility is caused by gas bubbles in the liquid hydraulic fluid.

The bulk modulus of an only slightly compressible liquid is dramatically reduced by the presence of a small volume of gas bubbles in the liquid (13). This tends to invalidate the assumption of incompressibility, limiting the usefulness of the hydraulic equation in modeling hydraulic control systems. And in addition to increasing the compressibility of a liquid, entrained gas decreases the fluid density, further invalidating the hydraulic equation.

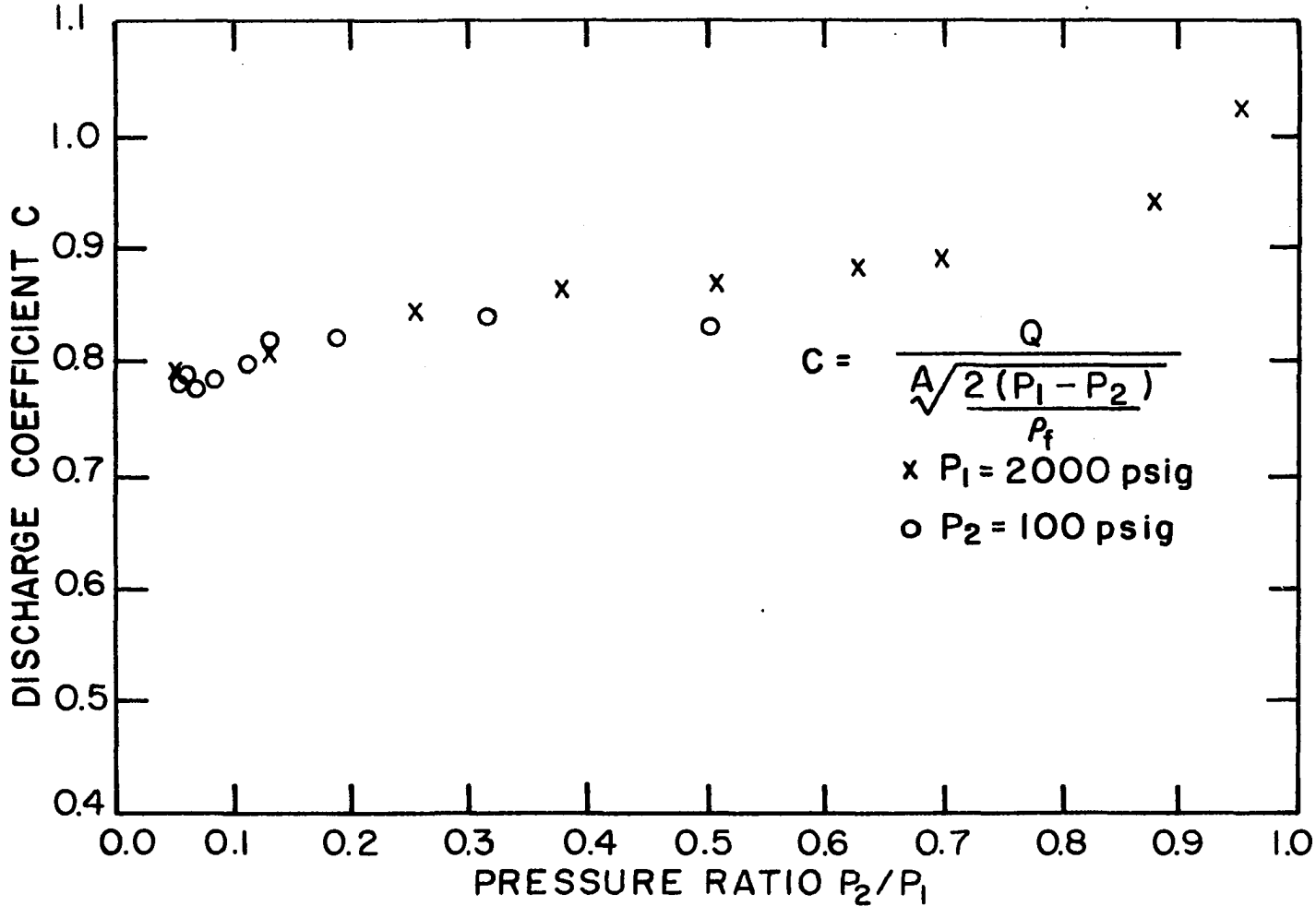

Figure 2. Selected results from tests by D. R. Storjohann

Unless special deaerators are used, every hydraulic system will contain some air (14). This may be present in the form of air trapped in high spots, as air entrained as bubbles, or as air dissolved in the oil. Some oils may retain air bubbles in the form of a foam, an emulsion of gas bubbles in the liquid. However, many hydraulic control system fluids contain foam destabilization agents (15), and the air can evidently rapidly transform from one form to another, eluding detection and measurement. Thus it was felt reasonable to believe that air was present in Storjohann's test system, and that this air was at least part of the reason for the observed anomalous flow characteristics. Other gases present might also include hydrocarbon vapors generated by cavitation of the liquid hydraulic fluid.

Flow rate through an orifice is governed by the pressure of the fluid at the vena contracta downstream of the orifice. In the tests conducted by Storjohann, and in similar tests conducted by McCloy and Beck (11) on a simulated spool valve, downstream pressure was measured in a cavity immediately downstream of the valve orifice, rather than at the flow vena contracta. This was necessary because there was no practical method available to measure pressure at the vena contracta, and because the results of such tests would be of more practical use in hydraulic system design. If the edges of the orifice are sufficiently sharp, the flow separates from the

confining walls at the orifice edges. If the flow remains separated downstream of the valve, the kinetic energy of the fluid is dissipated by turbulence, and the pressure in the downstream cavity is very nearly the same as the vena contracta pressure. McCloy and Beck (11) were able to observe that, under some conditions, the flow would reattach to one wall of the downstream cavity, causing some of the kinetic energy of the flow to be converted to pressure in the downstream cavity. This phenomenon is known as pressure recovery. Thus, under these conditions, the pressure measured in the downstream cavity was higher than the pressure at the vena contracta, and when the hydraulic equation was used to compute discharge coefficient for tests under these conditions, using downstream pressure for P_2, the resulting computed discharge coefficient was correspondingly high. It is believed that at least some of the variation in Storjohann's results at high pressure ratio was due to pressure recovery.

The reattachment of the flow downstream of an orifice is governed by the flow Reynolds number, which may be defined:

$$Re_x = \frac{Vl}{\nu}$$

where:

V=average fluid velocity at the orifice

l=orifice characteristic length, in this case chosen to be the distance between orifice edges

ν=fluid kinematic viscosity

In a study of spool valve orifice flow, Khokhlov (9) found discharge coefficient to be a function of Reynolds number. However, due to lack of information, the results of Khokhlov are not directly comparable to Storjohann's test results.

In their study of flow in a simulated spool valve, McCloy and Beck (11) found discharge coefficient to be a function of flow number, λ, which is defined by dividing Reynolds number by discharge coefficient at that Reynolds number:

$$Re_x = \frac{Vl}{\nu} = \frac{Ql}{A\nu}$$

From the hydraulic equation:

$$\frac{Q}{A} = C\sqrt{\frac{2(P_1-P_2)}{\rho_f}}$$

Thus:

$$Re_x = C\,\frac{l}{\nu}\sqrt{\frac{2(P_1-P_2)}{\rho_f}}$$

The flow number is then defined:

$$\lambda = \frac{l}{\nu}\sqrt{\frac{2(P_1-P_2)}{\rho_f}}$$

Test results presented in the form of discharge coefficient as a function of flow number are more directly useful to the hydraulic system designer since they allow a direct

computation of flow rate as a function of valve opening, upstream pressure, and downstream pressure. If discharge coefficient is presented as a function of Reynolds number, an iterative solution method is required to compute flow rate for a given valve opening, upstream pressure, and downstream pressure since Reynolds number is a function of flow rate, and thus discharge coefficient is itself a function of flow rate.

The results of McCloy and Beck (11) for incompressible flow indicate that discharge coefficient is a decreasing function of flow number λ, asymptotically approaching a constant value at high flow number (see figure 3). Flow numbers of the test points displayed in figure 2 were computed, and discharge coefficient plotted as a function of flow number in figure 4. In the case where upstream pressure was held constant, a similar trend was noted. This trend was not as pronounced in the case where the downstream pressure was held constant, even though the flow numbers were the same for both cases. It is believed that this is due primarily to the effects of compressibility of the fluid, since the entire range of pressure ratios was relatively low in the series of tests when downstream pressure was held constant.

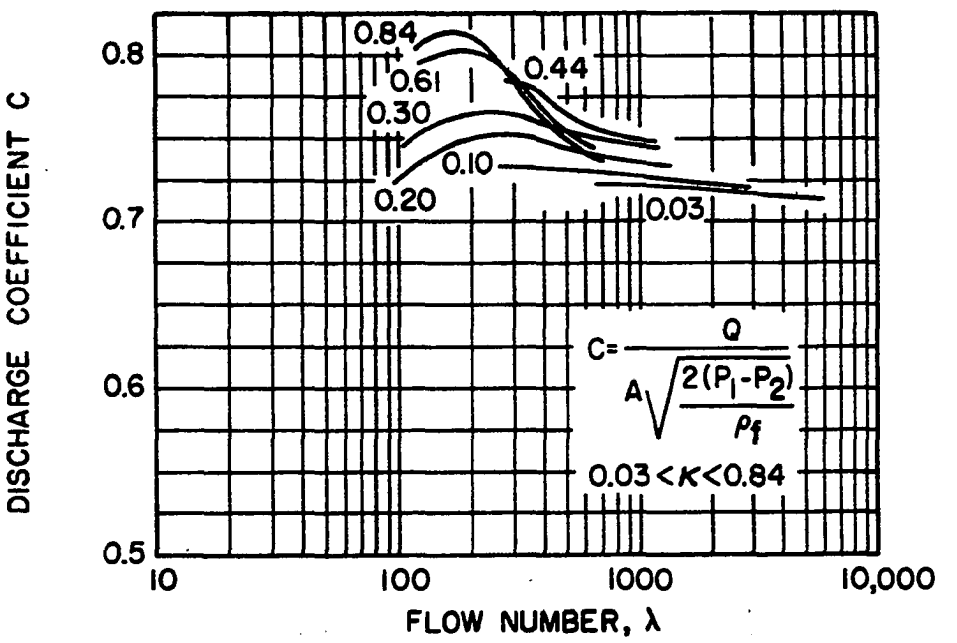

Figure 3. Results of McCloy and Beck--discharge coefficient vs. flow number

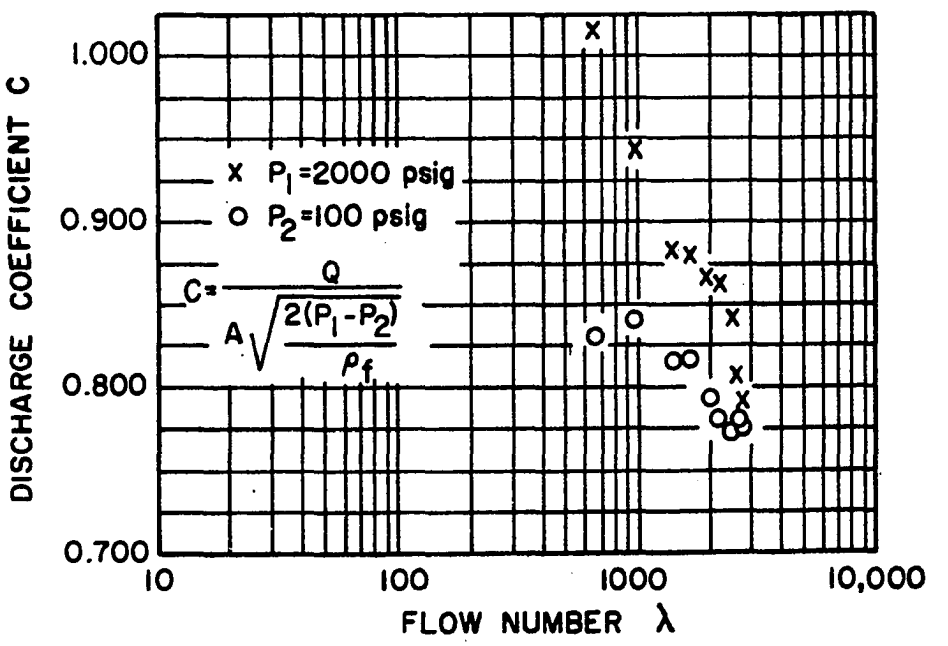

Figure 4. Results of Storjohann--discharge coefficient vs. flow number

THEORETICAL INVESTIGATION

Kays has proposed a homogeneous flow model utilizing single phase flow characteristics to predict two-phase flow pressure drop in an abrupt contraction in flow area (7,8).

Geiger (4) has reported a study of the flow of a two-phase fluid through a sudden contraction in duct area. Mass flow rate of a homogeneous mixture was found to correlate with pressure drop across a step contraction according to Kay's relationship:

$$\Delta P_c = \frac{G^2}{2\bar{\rho}}(K)$$

where:

ΔP_c=static pressure loss in steady flow of a fluid flowing through a sudden contraction in duct area

G=mass velocity of fluid in duct

$\bar{\rho}$=density of homogenous mixture of the liquid and gas phases

K=loss coefficient

This can be rewritten in a form similar to the hydraulic equation by noting that:

$$G = \frac{\bar{\rho}Q}{A}$$

where:

Q=volume flow rate through orifice

A=orifice area

Then:

$$\Delta P_c = \frac{\bar{\rho} Q^2 K}{2A^2}$$

or:

$$Q = \frac{1}{\sqrt{K}} A \sqrt{\frac{2\Delta P_c}{\bar{\rho}}}$$

Thus the term $\frac{1}{\sqrt{K}}$ is equivalent to C in the hydraulic equation. This equation can be rewritten in terms of the quality of the two-phase mixture and the properties of the two phases by noting that:

$$v = v_f + x v_{fg}$$

and:

$$v = \frac{1}{\bar{\rho}}$$

where:

v=specific volume of the two-phase mixture

v_f=specific volume of the liquid phase

v_{fg}=difference between the specific volume of the liquid phase and the specific volume of the gas phase

x=quality of the mixture, the ratio of the mass of the gas phase to the mass of the two-phase mixture contained in a volume of mixture.

Then:

$$Q = CA\sqrt{2(\Delta P_c)(v_f + xv_{fg})}$$

This can be further modified to a form more useful to the present analysis by noting that:

$$v_f + xv_{fg} = v_f\left[1 + x\frac{v_{fg}}{v_f}\right]$$

$$v_f = \frac{1}{\rho_f}$$

and:

$$Q = \dot{m}v$$

$$= \dot{m}(v_f + xv_{fg})$$

$$= \dot{m}v_f(1 + x\frac{v_{fg}}{v_f})$$

where:

$\dot{m}$=mass rate of flow through the orifice

The flow equation can then be rewritten:

$$\dot{m}v_f(1 + x\frac{v_{fg}}{v_f}) = CA\sqrt{2(\Delta P_c)v_f(1 + x\frac{v_{fg}}{v_f})}$$

or:

$$\dot{m}v_f = \sqrt{\frac{1}{(1 + x\frac{v_{fg}}{v_f})}} \quad CA\sqrt{\frac{2(P_1-P_2)}{\rho_f}}$$

For the purposes of this investigation it was assumed that the fluid consisted of air entrained in the hydraulic

fluid. The specific volume of the air may be determined by the ideal gas law:

$$v_g = \frac{RT}{P}$$

Thus:

$$v_{fg} = \frac{RT}{P} - v_f$$

and:

$$Q_\ell = CA\sqrt{\frac{2(P_1-P_2)}{\rho_f}}\sqrt{\frac{1}{1 + x\,\frac{\frac{RT}{P} - v_f}{v_f}}}$$

$$= CA\sqrt{\frac{2(P_1-P_2)}{\rho_f}}\sqrt{\frac{P}{P + x(\rho_f RT - P)}}$$

where Q_ℓ is the volume flow rate of the liquid phase through the orifice. This expression can be seen to be of the form of the hydraulic equation multiplied by a factor correcting for the effects of the gas phase. This factor is defined:

$$\Psi = \sqrt{\frac{P}{P + x(\rho_f RT - P)}}$$

so that:

$$Q_\ell = \Psi CA\sqrt{\frac{2(P_1-P_2)}{\rho_f}}$$

One assumption of Geiger's theoretical analysis was that the pressure drop across the sudden contraction was small compared to the fluid pressure. Since the two-phase fluid tested by Geiger was a steam-liquid water mixture, v_{fg} could be directly determined from steam tables, with the state defined by the fluid pressure at the orifice. However, the pressure drop in the test valve in the study reported herein varied from a small fraction of upstream pressure to nearly the entire upstream pressure. Thus it was necessary to evaluate the above correction factor at some intermediate pressure such that:

$$P = P_2 + \xi(P_1-P_2)$$

where ξ is an averaging factor defining the effective average pressure of the fluid as it flows through the orifice. Thus:

$$Q_\ell = C\Psi A\sqrt{\frac{2(P_1-P_2)}{\rho_f}}$$

and:

$$\Psi = \sqrt{\frac{P_2 + \xi(P_1-P_2)}{P_2 + \xi(P_1-P_2) + x(\rho_f RT - P_2 - \xi(P_1-P_2))}}$$

Orifice area, A, was computed based on Storjohann's hyperbolic area function (17):

$$A = \left[\frac{\pi D}{2}\right]\left[X + \sqrt{X^2 + M}\right]$$

where:

D=spool valve diameter

X=spool valve displacement from line-on-line

M=radial clearance factor (the theoretical value is 4 times the square of spool radial clearance)

With the additional assumption that there is no pressure recovery in the expansion downstream of the orifice, it is proposed to utilize this compressible flow model to describe the flow characteristics of the axial spool valve.

THE TEST PROGRAM

To determine the validity of the compressible flow model, the test valve developed by Storjohann (figure 1) was installed in the Fluid Power Laboratory, Mechanical Engineering Department, Iowa State University. The test valve has been described in detail by Storjohann (17). In summary, the valve consisted of a steel spool of one half inch nominal diameter, fitted in the steel valve body with radial clearance of 0.0003 inch. Both spool and body were constructed of hardened and tempered 8640 steel. The cylindrical surfaces of the spool were grooved circumferentially to balance pressure forces in the fluid leaking past the spool ends, so that the spool would tend to stay centered in the bore. Fluid momentum forces that would tend to decenter the valve were balanced by ensuring that the circumferential orifice slit was as uniform in width as possible. The metering edge of the spool was machined as nearly square as possible. The valve body was of split construction, with one surface of the split constituting the valve body metering edge, and this surface was ground to ensure flatness of the metering edge.

The spool position in the valve body was fixed by two micrometer screws, one at each end of the spool. The position of the spool metering edge relative to the valve body metering edge was measured by the micrometer on the downstream side of the spool, with a resolution of one ten thou-

sandth of an inch.

Since Storjohann's description, the valve has been modified somewhat. To eliminate the possibility of errors due to pressure drop in the lines, it was desired to measure the pressure upstream and downstream of the orifice in closer proximity to the orifice. Pressure taps were drilled in the inlet port and one outlet port, perpendicular to the port axes. The test valve body blocks were clamped together by four bolts. To ensure that the bolt preload was borne by the very rigid valve body blocks, rather than the less rigid "O" ring seals, the "O" ring glands were enlarged to allow for metal to metal contact at the valve body split.

Larger diameter clamping bolts were installed to ensure that bolt preload was maintained at high operating pressures. A torque indicating device was installed on the measuring micrometer to assist in obtaining consistent valve position measurements.

The hydraulic test circuit is depicted schematically in figure 5. The hydraulic power supply consisted of an axial piston pump driven by an electric motor. The pump circulated 80 gallons of American 303 fluid through the test apparatus at a rate of approximately 25 gallons per minute. Oil temperature was automatically regulated using a heat exchanger in conjunction with an electronic controller. In order to maintain a constant heat load on the controller, thus mini-

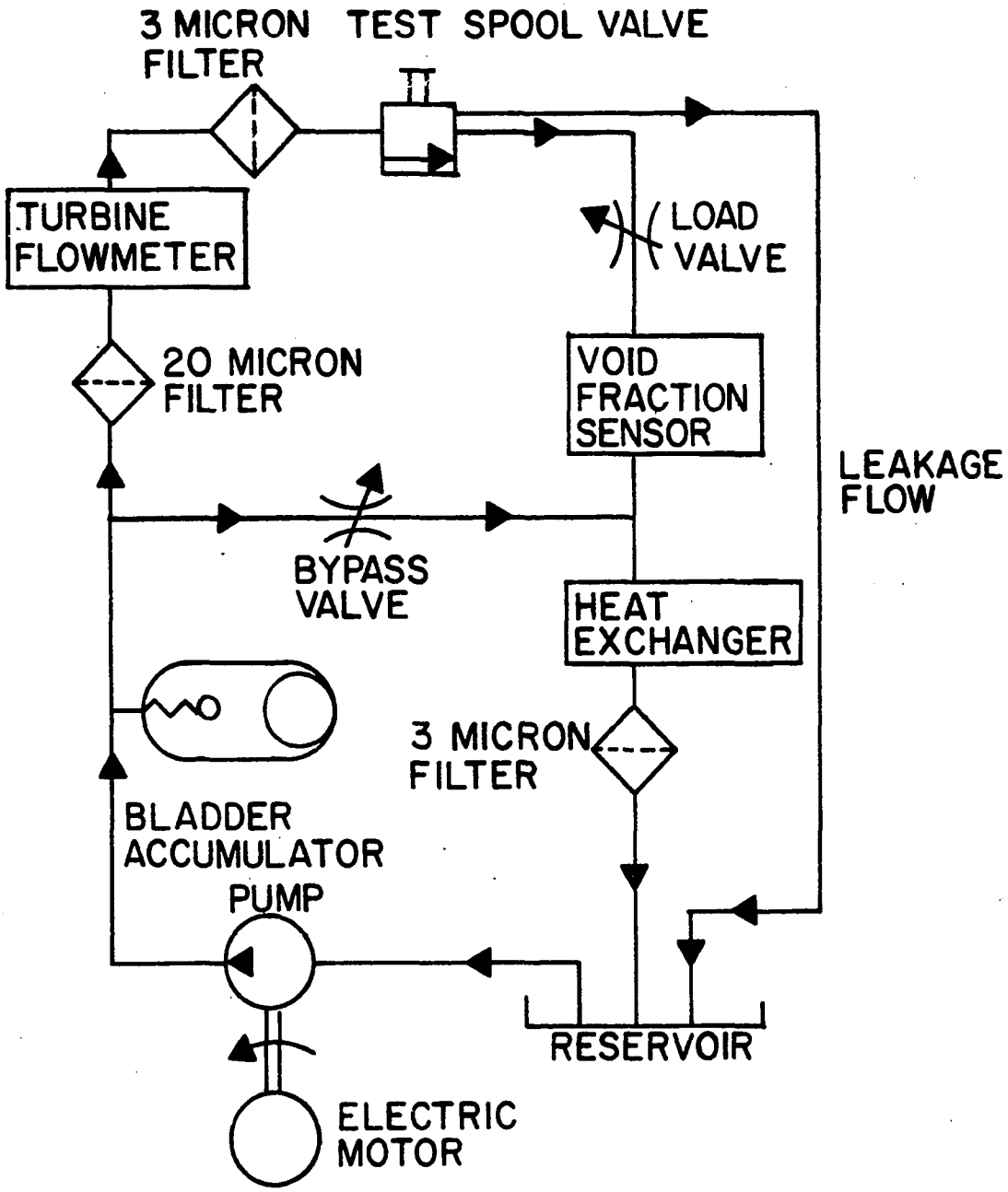

Figure 5. Diagram of hydraulic test circuit

mizing temperature fluctuation, the pump was operated at constant output pressure and constant flow rate. A needle valve was used to bypass surplus oil flow around the test valve to adjust the system for various fluid flow rates through the test valve, and a needle valve downstream of the test valve served as a load valve to adjust pressure downstream of the test valve.

An accumulator was used to smooth pressure pulsations in the pump output flow. The oil flowing through the test valve was passed through a 3 micron filter to eliminate undesirable effects that solid particles might have on the valve or on flow measurement.

Measurement Equipment and Procedures

The quantities measured were oil flow rate through the test valve orifice, pressures upstream and downstream of the valve orifice, spool valve position, and oil temperature.

Oil flow rate delivered to the valve assembly was sensed with a Cox model AN12 turbine flowmeter. This flowmeter was calibrated, using oil of the same type as the test fluid, at the John Deere Waterloo Tractor Works Product Engineering Center turbine flowmeter calibration facility. The flow rate at the sensor could then be determined with two measurements, flowmeter output frequency and fluid temperature. Flowmeter output frequency was determined with a Hewlett-Packard model 5211A electronic counter, periodically counting flowmeter

output pulses over a one second period. Fluid temperature was measured immediately downstream of the turbine flowmeter by means of a shielded thermocouple probe.

Flow through the turbine flowmeter was delivered to the test valve. A portion of this flow, Q_1, leaked through the spool valve radial clearance gap on the upstream side, thus bypassing the valve orifice. This leakage rate was measured by means of graduated cylinder and watch, and was subtracted from the turbine flowmeter measurement to determine the oil flow rate through the valve orifice. Leakage through the downstream clearance gap, Q_2, was routed back to the reservoir.

To ensure consistent pressure readings, pressures both upstream and downstream of the valve orifice were measured using the same Statham model PG731TC-2.5M-350 pressure transducer. Both upstream and downstream pressures were transmitted to a Pneu-Trol two section stack type gage isolator valve. The pressure transducer was mounted on the gage isolator valve, and either pressure could be applied to the transducer by depressing push buttons.

The transducer was of the unbonded strain gage type, used in conjunction with an Endevco model 4470 signal conditioner. An Endevco model 4476.2 Amplified Bridge Conditioner mode card provided voltage regulated excitation, means for balancing and calibrating the transducer, and also amplified

the transducer output. Readout was accomplished with an API model 4304 digital panel meter.

With the gage isolator pushbuttons in normal position, atmospheric pressure was applied to the pressure transducer. Before a pressure reading was taken, the signal conditioner amplifier was zeroed and the transducer strain gage bridge balanced, eliminating various forms of drift from the subsequent readings. Then overall measurement system sensitivity was checked using a calibration resistor in parallel with one element of the transducer strain gage bridge, unbalancing the bridge a precise amount. Then signal conditioner amplifier gain was adjusted until system output read a certain value, previously determined by calibration. After this procedure, the pressure measurement system would read directly in psi at the pressure corresponding to the calibration output, and at zero gage pressure. Other pressure readings were corrected for system non-linearity by previously determined dead weight tester calibration. Calibration was checked periodically throughout the test program, without significant change being detected.

Valve position, relative to the valve body, was measured by a 0.0001 inch resolution micrometer. To determine X_0, the micrometer reading at X=0 (spool edge flush with lower valve body face), a flat ground plate was constructed with a key-hole shaped slot, so that the narrow section of the slot was

somewhat narrower than the spool diameter, but would accommodate the waist of the spool. This plate was then clamped between the upper and lower valve body blocks, so that the spool was free to move down to X=0, but no further. The clamping bolts were carefully tightened to preload torque, the spool was advanced to the plate, and the micrometer zero reading was recorded. The plate was then removed, and the clamping bolts carefully retightened to the preload torque.

An attempt was made to measure the amount of gas entrained in the hydraulic fluid while the fluid was flowing in the line. It was felt that measuring the gas content in line would eliminate errors that would result from drawing a sample and evaluating it at pressure and temperature different from test conditions.

The sensor, which was located approximately six feet downstream of the test valve, consisted of a coaxial capacitor, with the fluid flowing axially through the annular duct between the two coaxial capacitor elements. The fluid acted as the capacitor dielectric, and sensor capacitance was an approximately linear function of fluid void fraction (1).

A Tektronix Type Q Transducer and Strain Gage Bridge was used to measure capacitance shifts of the sensor in such a way that bridge unbalance (and thus Type Q unit output voltage) was proportional to the void fraction of the fluid in the sensor. To obtain maximum sensitivity for measuring

small quantities of entrained air, an external bridge was used with four resistive arms of 1000 ohms each. The sensor was connected in parallel with one arm of the bridge, and fixed value capacitors were added in parallel to an adjacent arm of the bridge so that the bridge would be approximately balanced when the sensor was filled with deaerated oil. Final resistive and capacitive balance was achieved with fixed and variable capacitors available internally in the Type Q unit.

In the use of the sensor, it was assumed that the gas consisted of air only. The test oil was passed through the sensor until the sensor reached thermal equilibrium, and then the sensor was filled with vacuum deaerated oil at the test temperature. The measurement system was zeroed, then the sensor drained and system output noted. This output corresponded to 100% void, and calibrated the transducer for the test temperature. The void fraction during subsequent tests could be determined by the ratio of measurement system output voltage during the test to this calibration output.

Total dissolved air content of the hydraulic fluid was measured using a Seaton-Wilson Model AD 4003 Aire-Ometer. A measured quantity of test oil was drawn into the Aire-Ometer at atmospheric pressure. The oil was then distributed in a thin film inside the Aire-Ometer and subjected to a vacuum, removing the dissolved air from solution. Then the sample

was repressurized to atmospheric pressure, and the volume of gas noted. Since the volume occupied by a given mass of air depends on sample temperature, and several minutes time was required to complete a dissolved air content test, the test was conducted with the Aire-Ometer and oil sample at room temperature, rather than at flow test temperature, so that sample temperature would not change significantly during the test.

Fluid temperature within the void fraction sensor was measured with an iron-constantan thermocouple used in conjunction with a Leeds and Northrup Voltage Balancing Potentiometer.

Acquisition of Data

At small valve openings, the determination of discharge coefficient was very sensitive to the measurement of valve position. The measurement of valve position by micrometer was affected by the temperature distributions within the valve body and the micrometer. Thus care was exercised to conduct the tests at as near thermal equilibrium as possible to obtain maximum consistency in valve position measurement. The valve body was covered, as completely as possible, with styrofoam insulation of two inch thickness, and tests were conducted with constant flow rate so that the heat input rate to the valve would be as constant as possible.

The spool was positioned at the desired opening for the initial test point, and the system warmed up with maximum pressure drop across the test valve. The valve position measuring micrometer reading was checked periodically during warmup, and upstream pressure was maintained at 2000 psi throughout the tests. The test apparatus was allowed to reach thermal equilibrium, and the measurements were taken.

Subsequent test points, at different valve openings and downstream pressures, were obtained by advancing the spool valve positioning micrometer to the desired valve opening, and closing the load valve until upstream pressure again read 2000 psi. If flow rate had changed, the bypass valve was re-adjusted, although this was seldom necessary. The system was operated at the new test point until the new thermal equilibrium had been reached.

As soon as the desired test conditions were obtained, measurements were taken, and the system readjusted for the next test point. The oil temperature regulation system allowed temperature variations on the order of one degree Fahrenheit, but these were of a relatively rapidly varying nature, compared to the apparent thermal time constant of the test valve.

After the series of test points, some of the initial test points were repeated. If the valve position readings corresponding to the pressure drop measurements had shifted

measurably, the series of test points was repeated. When it was found necessary to repeat the tests, thermal equilibrium had by that time been approached sufficiently close that the second series of tests was repeatable.

When a satisfactory series of test points had been obtained, the test apparatus was readjusted for the next flow rate, and the above procedure repeated.

The conditions governing leakage through the upstream spool radial clearance gap were maintained nearly constant, and variation in leakage rate was found to be insignificant. Therefore it was found to be necessary to measure leakage rate only occasionally.

TEST RESULTS AND DISCUSSION

Preliminary tests indicated that the amount of gas entrained in the test oil as it flowed through the capacitive void fraction sensor was so small as to be immeasurable. This indicated that if gas was present in the fluid as it flowed through the valve orifice, causing the anomalous test results, it had condensed or returned to solution by the time it reached the void fraction sensor. Since the test valve assembly was constructed of steel, it was not possible to observe the flow in or downstream of the orifice to determine with certainty what occurred.

In order to simulate the spool valve flow of the test fluid in a situation in which it could be observed, a small globe valve was fitted with several feet of transparent plastic tubing downstream of the valve. Hydraulic fluid at test conditions was pumped through the valve at various upstream pressures for various valve openings. Downstream pressure was maintained near atmospheric pressure due to strength limitations of the plastic tubing. Under certain conditions, the flow immediately downstream of the valve was seen to be translucent, due to bubbles in the fluid. These bubbles would disappear within a few inches of the valve, as long as the fluid was flowing.

It is believed that the observed bubbles were air, since they would persist for a time if the flow was suddenly halt-

ed, rather than immediately disappear as would be expected if the bubbles were hydrocarbon vapor produced by cavitation. It is possible, however, that cavitation did take place within the valve, where it could not be observed, and that the hydrocarbon vapor bubbles so generated had condensed within the valve before entering the transparent tubing. Further, the observed bubbles may have contained a significant portion of hydrocarbon vapor in addition to air. The stationary fluid on the downstream side of the valve would initially appear translucent, due to the bubbles entrained in the fluid, but would gradually clear as the bubbles slowly dissolved or coalesced into larger bubbles.

Also, it is believed that the bubbles formed as the fluid flowed through the orifice. Two of the factors which cause bubbles to dissolve are pressure and fluid motion (3). The pressure was much higher upstream of the valve, and fluid velocity was approximately the same as downstream of the valve, so there is little reason to believe that there were bubbles present upstream of the valve if the bubbles disappeared so quickly while flowing on the downstream side of the valve.

Similar observations were reported by McCloy and Beck (11) in their study of effects of cavitation in spool valve orifices. Their test apparatus consisted of a two-dimensional slot with variable opening width, constructed of Per-

spex so that the flow could be observed and photographed. Tests were conducted to determine conditions of incipient cavitation using both water and Shell Tellus 27 oil.

In this study, cavitation was detected acoustically as a crackling sound. Pressure upstream of the test valve was initially set sufficiently low that no cavitation took place. They report that, as upstream pressure was increased, a white line was seen to form along one edge of the downstream side of the orifice. This was interpreted as "deaeration" since the crackling sound characteristic of cavitation was not detected and the appearance of the oil downstream of the orifice suggested gas bubbles.

As upstream pressure was increased further, deaeration increased, and eventually cavitation set in. No mention was made of the persistence of the bubbles. No attempt was made to determine the air content of the oil, nor was any attempt made to measure the amount of gas evolved from the fluid.

In a study of critical flow of two-phase fluid, Henry (6) implicated gases coming out of solution as the cause of acceleration of liquid water, at pressures above saturation, in a constant area duct. Further, he suggests that if the fluid pressure is near the saturation pressure, a bubble at 100% relative humidity would be almost entirely water vapor. This implies that the amount of gas dissolved in a liquid might have a much greater effect on flow characteristics than

could be accounted for by the evolution of the dissolved gas from solution. Henry made no attempt to deaerate his test fluid, but Zaloudek (20) reported that decreasing the air content of test fluid in a similar study resulted in an increased critical flow of 5 - 8 %.

In their study of incipient cavitation in spool valve orifices, McCloy and Beck (11) defined cavitation number κ, which is a measure of the tendency of the flow to cavitate, such that:

$$\kappa = \frac{P_2 - P_v}{P_1 - P_2}$$

where P_v is the fluid vapor pressure. Flow number λ was defined:

$$\lambda = \frac{l}{\nu}\sqrt{\frac{2(P_1-P_2)}{\rho_f}}$$

where l is a characteristic length. Tests were undertaken to determine values of κ at which cavitation was incipient for various λ. Results of tests using two different fluids, oil and water, are shown in figure 6 for incipient cavitation, in their simulated spool valve. κ_i, the value of κ at incipient cavitation, is plotted for various flow number. At a given flow number, κ less than κ_i indicates cavitation, and κ greater than κ_i indicates lack of cavitation.

Discharge coefficient, as defined by the hydraulic equation, is plotted in figure 8 as a function of pressure ratio

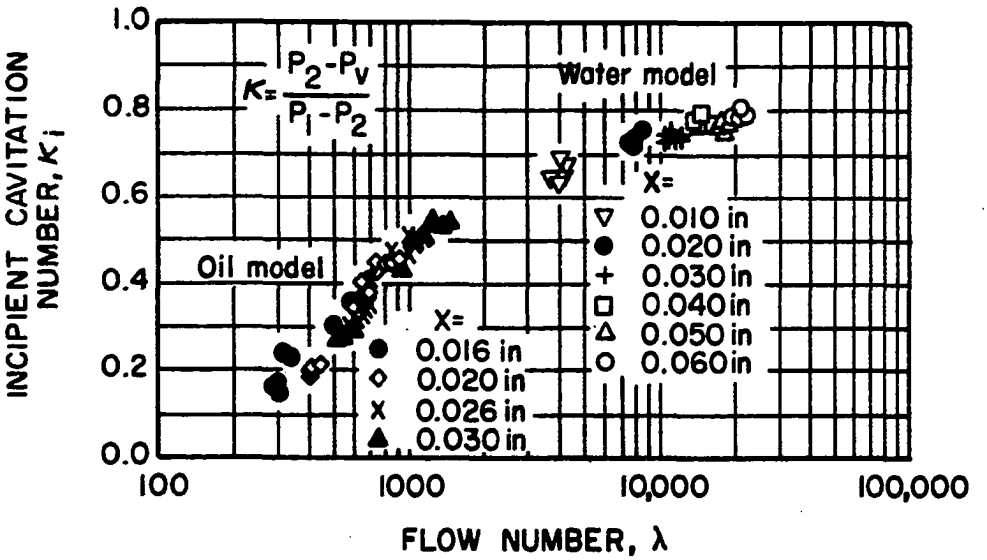

Figure 6. Results of McCloy and Beck--incipient cavitation number vs. flow number

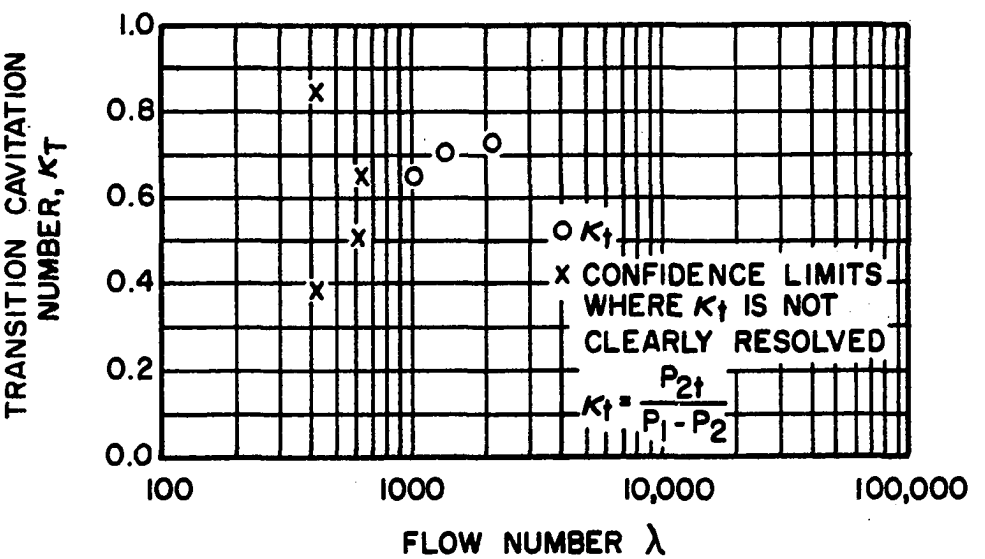

Figure 7. Test results--transition cavitation number vs. flow number

for one flow rate measured by the author. It is seen to be an increasing function of pressure ratio at low values of pressure ratio, rather than the expected constant. At a certain transition pressure ratio, discharge coefficient is seen to drop suddenly to a lower value, and remain approximately constant for higher pressure ratios. The transition pressure ratio is an increasing function of flow rate, becoming more sharply defined at higher flow rates.

Above the transition pressure ratio, the relatively constant discharge coefficient indicates that the flow is characteristic of incompressible flow, and below the transition pressure ratio the flow is more characteristic of compressible flow. It is believed that the transition is one such that the fluid remains liquid at greater pressure ratios, but that deaeration and cavitation take place at lower pressure ratios, causing the fluid to become compressible as it flows through the orifice.

Also plotted in figure 7 are values of κ at the transition pressure ratios of the tests reported herein, at their corresponding values of λ. The fluid vapor pressure was not known exactly, but it was known to be small compared to P_2 at the transition value of P_2. Thus transition κ, or κ_t, is defined:

$$\kappa_t = \frac{P_{2_t}}{P_1 - P_{2_t}}$$

where P_{2_t} is the value of pressure downstream of the orifice at transition. Flow number λ was computed in a manner similar to that used by McCloy and Beck, using valve opening as the characteristic length, l.

Figure 7 shows that κ_t follows the same general trend as κ_i did in the results of McCloy and Beck, but that κ_t is somewhat higher in value. McCloy and Beck mentioned that deaeration of the fluid occurs at values of κ higher than κ_i, and it is believed that the transition noted in the study reported herein occurs due to deaeration. McCloy and Beck did not report values of κ for incipient deaeration. However, McCloy and Beck did report the belief that results of a study of incipient cavitation reported by MacLellan, Mitchell, and Turnbull (12) are 20% too high, based on the assumption that they were observing incipient deaeration rather than incipient cavitation. Reducing by 20% the values of κ_t shown in figure 7 would cause the data points to fall among those reported by McCloy and Beck.

It was not possible in the tests reported herein to distinguish by ear between deaeration and cavitation, since the background sound level due to the hydraulic power supply was much greater than the sound transmitted by the flow from within the thickly insulated valve.

A small part of the difference in results is due to difference in test procedure. Incipient cavitation, as reported

by McCloy and Beck, is noted at the transition from flow not cavitating ($\kappa > \kappa_i$) to flow cavitating ($\kappa < \kappa_i$), with κ decreasing throughout the test. Due to the sequence of data acquisition, results reported herein are for desinent conditions, which are noted at the transition with κ increasing. Some hysteresis generally occurs, so that desinent cavitation occurs at a somewhat higher cavitation number than incipient cavitation.

The similarity between the results of McCloy and Beck (11) and the results reported herein suggests that the transition from the high pressure ratio flow regime to the low pressure ratio flow regime is due to the formation of a compressible gas phase which modifies the flow characteristics. This suggests defining discharge coefficient for the low pressure flow regime using the compressible flow model described above:

$$C = \frac{Q_\ell}{\Psi A \sqrt{\frac{2(P_1-P_2)}{\rho_f}}}$$

where:

$$\Psi = \sqrt{\frac{P_2 + \xi(P_1-P_2)}{P_2 + \xi(P_1-P_2) + x(\rho_f RT - P_2 - \xi(P_1-P_2))}}$$

It is believed that the amount of gas evolving from the liquid depends on the pressures upstream and downstream of the

valve. The initial analysis of the data indicated that, for a given flow rate, the amount of gas required to result in a constant discharge coefficient as computed from the data by the above equation was a linear function of pressure ratio. It was believed that at or near transition, very little gas was evolved, but as pressure ratio was lowered from the transition value, additional gas was evolved. Since it was not possible to measure the exact quality of the fluid flowing through the orifice, this is accounted for empirically in the compressible flow model by assuming that:

$$x = x_0 - a(P_2/P_1) \qquad \text{for } \kappa<\kappa_t$$

$$x = 0 \qquad \text{for } \kappa>\kappa_t$$

Then the compressible flow definition of discharge coefficient becomes:

$$C = \frac{Q_\ell}{\Psi A\sqrt{\frac{2(P_1-P_2)}{\rho_f}}}$$

where:

$$\Psi = \sqrt{\frac{P_2 + \xi(P_1-P_2)}{P_2 + \xi(P_1-P_2) + (x_0-a(P_2/P_1)(\rho_f RT-P_2-\xi(P_1-P_2))}}$$

for $\kappa<\kappa_t$.

McCloy and Beck (11) found discharge coefficient to be a function of flow number for non-cavitating flow. To determine the compressible flow characteristics of the valve tested, and compare these characteristics to those determined by

McCloy and Beck, that test data above transition pressure ratios was first analyzed separately.

The test data reported herein were obtained by varying valve opening and downstream pressure while holding flow rate and upstream pressure constant. This is approximately equivalent to maintaining flow number constant, so that if the discharge coefficient of incompressible flow is a function only of flow number, it should be approximately constant for a given flow rate. A least squares curve fit procedure was used to determine the optimum values of the parameters X_0 and M, and one discharge coefficient for each of the five test flow rates, which would best describe the incompressible flow results in terms of the hydraulic equation. This procedure selected values of the parameters which minimized the sum of the squared differences between discharge coefficients measured at the test points and the corresponding parameter discharge coefficients.

In the derivation of his hyperbolic orifice area equation, Storjohann determined that, in theory, the value of M should be four times the square of the valve spool radial clearance. By micrometer he determined that the average radial clearance was 0.00029 inch. Thus the value of M was expected to be 0.000000336. However, in the analysis of his data, he found the value of M giving optimum least squares curve fit to be 0.00000096, which is roughly three times the

expected theoretical value, and equivalent to a spool radial clearance of 0.00049 inch. The analysis of the data reported herein determined the optimum least squares curve fit to be obtained with a value of M of 0.00000026. This is equivalent to a radial clearance of 0.000255 inch, quite close to the measured value of 0.00029 inch.

Figure 9 shows the measured discharge coefficients as evaluated using the optimum parameters $\bar{x}_0$ and M determined by the least squares curve fit procedure. Results are shown for five flow rates. Both measured discharge coefficient and flow number are seen to vary somewhat for a given flow rate. The general trend is similar to that observed by McCloy and Beck, with discharge coefficient decreasing as a function of flow number, asymptotically approaching a constant value at high flow number.

Although the results shown in figure 9 are similar to those reported by McCloy and Beck, the results do not indicate a smooth curve connecting the discharge coefficients between flow rates. It is believed that this is due to errors in measurement of valve opening caused by differences between the thermal expansions of the spool and the valve body.

The test valve was insulated to aid in obtaining a uniform temperature within the test valve assembly. The spool valve and valve body were constructed of the same material to minimize variations due to differences in thermal expansion.

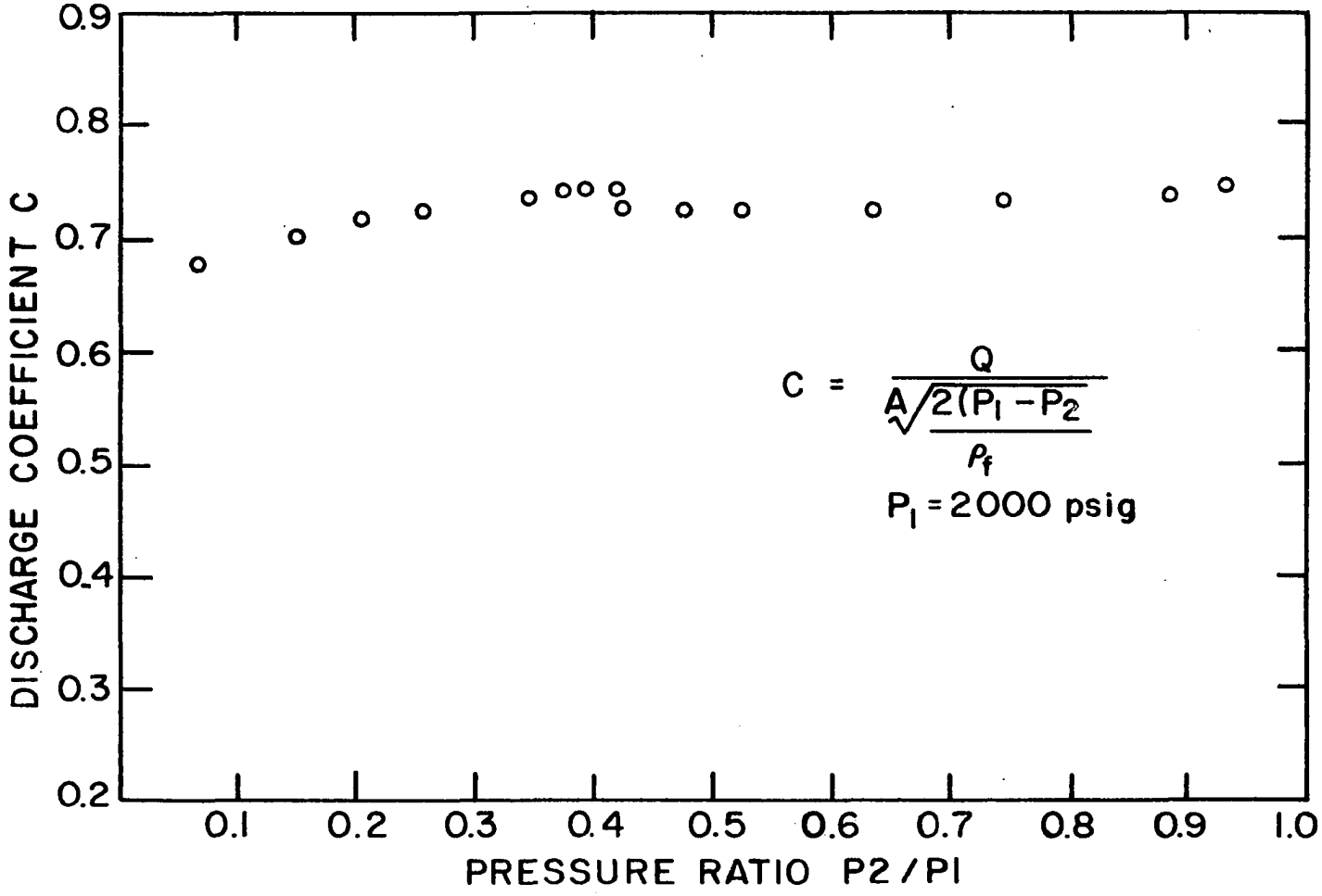

Figure 8. Discharge coefficient vs. pressure ratio for a fixed flow rate.

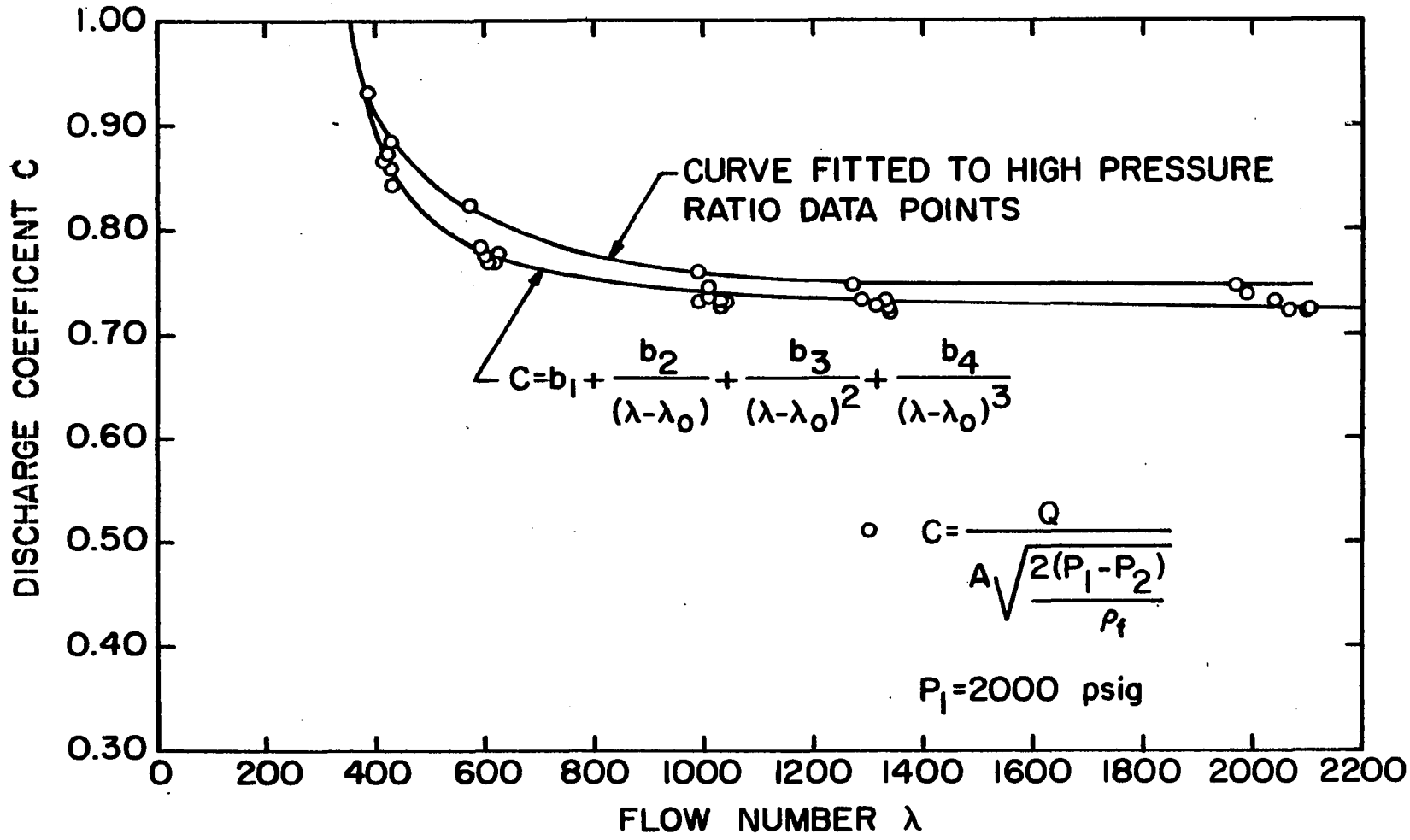

Figure 9. Discharge coefficient vs. flow number for incompressible flow regime

Individual test runs were conducted with fluid flow rate held constant in order to maintain heat input as constant as possible, and the test valve was allowed to reach thermal equilibrium before readings were taken.

However, the throttling effect of the valve raises the temperature of the oil downstream of the orifice, varying from an insignificant amount when pressure drop across the valve is small (high pressure ratio) to an estimated $20^{o}F$ for large pressure drop. The highly turbulent flow in the downstream cavity transfers heat very rapidly to the spool and to the valve body. When pressure drop is changed, the new heat transfer rate to the valve body causes it to assume a new temperature distribution. This temperature distribution is affected by the pressure drop across the orifice, the flow rate through the test valve, and the radial clearance gap leakage flow. With a given set of test conditions, the temperature within the valve body varies from close to downstream oil temperature at the downstream cavity to inlet oil temperature at the inlet port. The only temperatures measured within the valve body during testing were the temperatures of the upstream and downstream leakage flows, after the fluid had been throttled to atmospheric pressure. As testing progressed, these temperatures were found to be very nearly constant, indicating that the leakage was being cooled by the surrounding valve body and that the temperature distribution

over much of the downstream half of the valve body was not greatly affected by the higher downstream fluid temperature when downstream pressure was low. However, much of the downstream half of the spool is immersed in the flow in the downstream cavity, and, it is believed, the downstream half of the spool undergoes a much greater change in average temperature than does the valve body, causing a differential expansion.

Since the micrometer spindle was immersed in the downstream leakage flow, which was of quite constant temperature during the tests, it is believed that little error was caused by expansion of the micrometer while testing was in progress. However, in warming the valve from room temperature, where the micrometer was calibrated for valve line-on-line reading, to test temperature, considerable differential expansion was encountered. It was noted that when the test valve had cooled after a test and the final valve position reading was repeated without having changed the positioning micrometer, as much as 0.0006 inch difference would be noted. This quantity is not suitable for use as a calibration since it involves expansion of many other elements of the system, but it is indicative of the order of magnitude of valve position measurement shifts encountered. The warm up expansion negates the ground plate calibration of the measuring micrometer for spool line-on-line reading.

Assuming that the valve position measuring micrometer read consistently (regardless of flow rate) when there was little pressure drop across the valve (and thus a quite uniform temperature distribution within the entire insulated valve assembly), the thermal expansion effects due to a greater pressure drop (lower pressure ratio) would cause the micrometer to indicate a greater valve opening than was actually the case.

For a test point at low pressure ratio (high pressure drop), the valve would not be as far open as the micrometer reading would indicate. This would cause the area term in the denominator of the discharge coefficient function to be larger than the actual orifice area, and the resulting computation of discharge coefficient to be smaller than the actual discharge coefficient at that test point. This error would range from negligible at high pressure ratio to a maximum at low pressure ratio. The percentage error in discharge coefficient caused by an error in valve position measurement is a decreasing function of valve opening since the error in orifice area becomes smaller relative to the actual orifice area. Also, it is suspected that since higher flow rates transfer more heat to the valve body, it more nearly approaches the temperature distribution of the spool, decreasing the differential in expansion.

With the assumption of negligible error at high pressure ratios, a smooth curve may be fitted to the high pressure ratio incompressible flow points for each flow rate, as in figure 9. This curve is similar to the results of McCloy and Beck (11) for non-cavitating flow.

The results for test points at lower pressure ratios indicate that the discharge coefficient decreases with decreasing pressure ratio (κ decreasing), deviating from the curve fitted to the high pressure ratio points. This deviation is less for tests conducted at high flow number (thus high flow rate).

The results shown in figure 9 are for tests run with λ held approximately constant, but κ varying. McCloy and Beck display results with κ held constant, and λ varying. Under these conditions, their results indicate discharge coefficient increasing slightly with decreasing κ, the opposite of the effect noted above. The results reported by McCloy and Beck are believed to be quite accurate, since they are based on valve position measurements obtained directly by optical methods.

Thus the deviations from previously published results suggest that errors were introduced by variations in thermal expansion of the valve assembly.

The differential thermal expansion effect may be expected in any axial spool valve installation, the net effect of

the differential expansion depending on the construction of the valve body, especially port location. The significance of these tests is that they determine steady state flow characteristics of a spool valve as a function of position of the downstream end of the spool, rather than as a function of valve opening. The main thermal effect would be on steady state operating conditions since the differential expansion requires several minutes to reach equilibrium. There would be little effect on oscillatory instabilities, so the hydraulic control system designer would benefit from information concerning flow based on instantaneous orifice opening, rather than steady state orifice opening.

The effect of the gas entrained in the fluid is basically to decrease the flow discharge coefficient from what would be expected for liquid flow. It is impossible to distinguish between the variation in measured discharge coefficient due to entrained gas and that variation due to thermal expansion effects. For test points at low values of flow number, the variation due to flow number related effects further masks the effects of the entrained gas.

To evaluate the effects of the gas phase, it was first assumed that C would be basically the same function of flow number that resulted from incompressible flow, and that the remaining variation in C would be accounted for by two-phase flow effects. By a least squares curve fit procedure, a

smooth curve was fitted to the incompressible flow discharge coefficient results, of the form:

$$C = b_1 + \frac{b_2}{(\lambda - \lambda_0)} + \frac{b_3}{(\lambda - \lambda_0)^2} + \frac{b_4}{(\lambda - \lambda_0)^3}$$

The values of the parameters for optimum curve fit of an equation of this form were found to be:

λ_0=179.56

b_1=0.711711

b_2=22.75134

b_3=668.0791

b_4=763810.3

Then, based on the values of X_0 and M determined as optimum for describing the incompressible flow results, the optimum compressible flow parameters x_0, a, and ξ were determined by least squares curve fit for each of the flow rates tested. An additional factor, δ, was utilized to account for the noted higher discharge coefficient under compressible flow conditions. Discharge coefficient for pressure ratios below transition was defined:

$$C_c = C + \delta$$

where:

C=incompressible flow discharge coefficient, a function of flow number

δ=increment of increase in discharge coefficient at

transition from incompressible to compressible flow conditions

C_c=compressible flow discharge coefficient

It was found that there was very little effect due to compressibility in the data sets at low flow number (low flow rates), and that there was increasing effect due to compressibility at high flow numbers. The parameters x_0 and a were found to be directly proportional to flow number (figures 10 and 11). To develop a universal expression for the flow characteristics of the fluid, the expressions for the parameters x_0 and a were defined:

$$x_0 = \beta\lambda$$

$$a = \alpha\lambda$$

and the entire data set was analyzed by least squares method to find the optimum values of α, β, δ, and ξ. These were found to be:

α=0.00002779

β=0.00001171

δ=0.0202

ξ=0.4278

Results are shown in figure 12 utilizing the incompressible flow model to compute discharge coefficient for test points at pressure ratios greater than the transition pressure ratio, and using the compressible flow model for test points at pressure ratios less than the transition value.

Results are also tabulated in Table 1, along with an estimated confidence limit for each measured discharge coefficient. Confidence limits were estimated based on estimated error limits of two psi for the pressure measurements, and one least count for all other measurements. The estimate was evaluated by ISU CADET algorithm program ME0230, which evaluates the propagation of error equation (2) by finite difference techniques. For reference, figure 13 shows results evaluated by the incompressible model (hydraulic equation) only.

The compressible flow model was based on Kays' model of homogeneous two-phase flow through a sudden contraction in duct area, which was intended for the case where the two phases would be uniformly mixed as they enter the valve orifice, and the pressure drop across the valve orifice would be small compared to the static pressure downstream of the valve. In the tests conducted, the gas evidently evolved from the liquid as it flowed through the orifice, and the pressure drop across the valve varied from a small fraction of the downstream static pressure to several times the downstream static pressure. However, the compressible model, with compensating alterations of Kays' model, describes the low-pressure-ratio flow regime more satisfactorily than does the hydraulic equation.

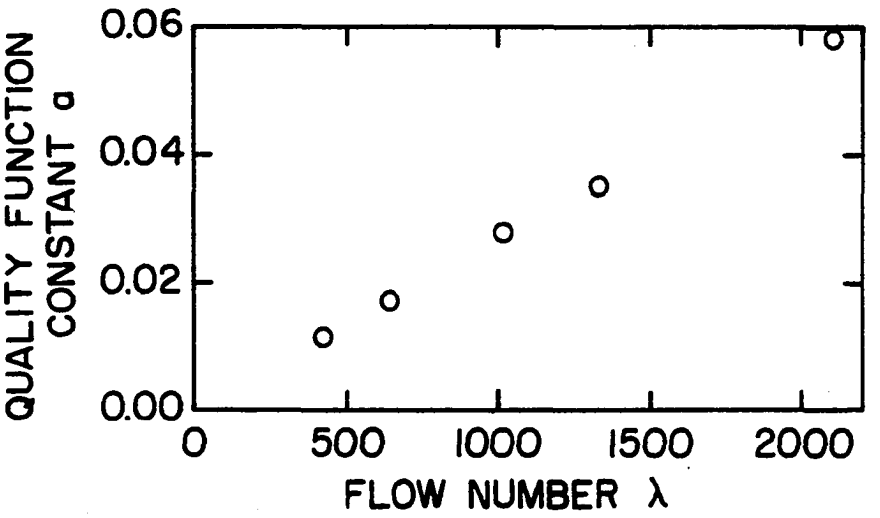

Figure 10. a vs. flow number

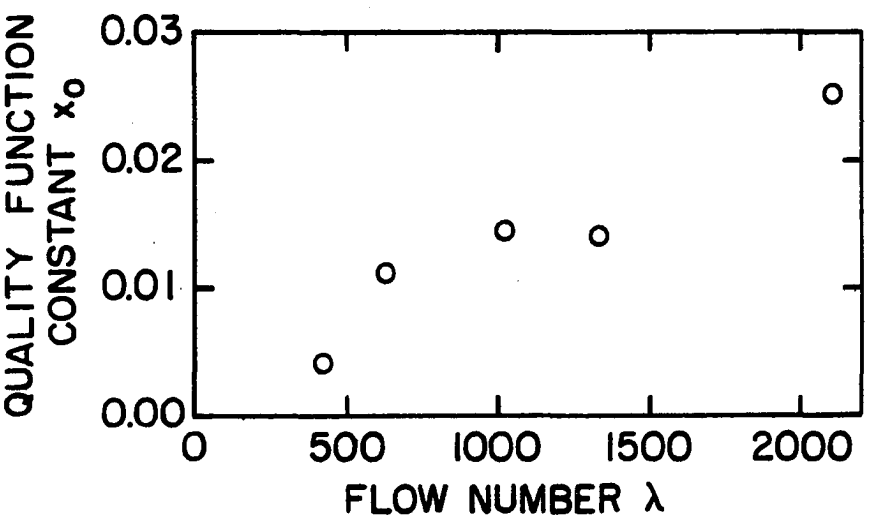

Figure 11. x_0 vs. flow number

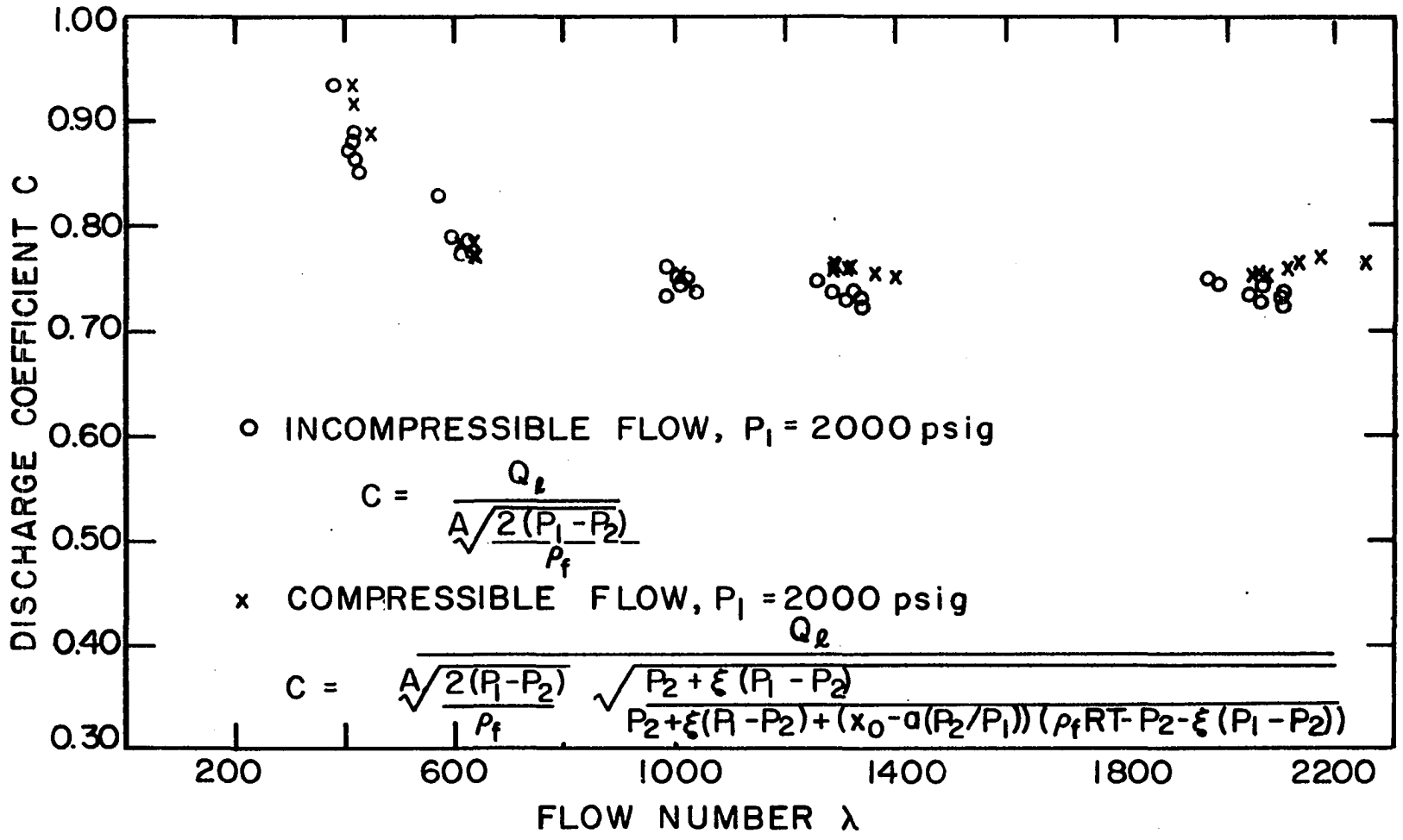

Figure 12. Discharge coefficient vs. flow number for both compressible and incompressible flow regimes

Table 1. Confidence limits of discharge coefficients

Pressure Ratio	Flow Number	Discharge Coefficient	Limit of Confidence From Measured Value
Flow Rate Number 1			
0.0239	451	0.8851	0.0602
0.2753	415	0.9306	0.0596
0.3437	420	0.9012	0.0546
0.4586	426	0.8871	0.0490
0.5819	421	0.8748	0.0425
0.7216	427	0.8584	0.0342
0.8131	430	0.8448	0.0277
0.8997	414	0.8658	0.0226
0.9547	387	0.9308	0.0226
Flow Rate Number 2			
0.0264	640	0.7650	0.0371
0.1378	641	0.7846	0.0364
0.2056	640	0.7817	0.0347
0.2803	632	0.7760	0.0331
0.3393	632	0.7758	0.0318
0.3931	627	0.7739	0.0306
0.4883	618	0.7714	0.0284
0.5863	622	0.7793	0.0260
0.6858	608	0.7775	0.0231
0.7739	600	0.7789	0.0199
0.8571	596	0.7830	0.0166
0.9326	573	0.8247	0.0151
Flow Rate Number 3			
0.0343	1024	0.7374	0.0230
0.1491	1025	0.7471	0.0220
0.2442	1018	0.7454	0.0208
0.3269	1014	0.7506	0.0198
0.3922	1009	0.7369	0.0185
0.4784	990	0.7307	0.0172
0.6299	1043	0.7320	0.0143
0.7080	1034	0.7316	0.0130
0.7987	1031	0.7319	0.0110
0.8750	1007	0.7449	0.0097
0.9427	993	0.7578	0.0112

Table 1. Continued

Pressure Ratio	Flow Number	Discharge Coefficient	Limit of Confidence From Measured Value
Flow Rate Number 4			
0.0833	1398	0.7499	0.0175
0.1685	1363	0.7511	0.0172
0.2516	1322	0.7573	0.0169
0.2967	1310	0.7592	0.0166
0.3482	1289	0.7646	0.0164
0.3728	1291	0.7602	0.0160
0.3989	1290	0.7556	0.0156
0.4348	1327	0.7334	0.0143
0.5264	1332	0.7288	0.0130
0.5967	1337	0.7258	0.0119
0.6527	1341	0.7234	0.0111
0.7962	1315	0.7266	0.0089
0.8774	1289	0.7339	0.0081
0.9407	1264	0.7469	0.0102
Flow Rate Number 5			
0.0673	2249	0.7580	0.0116
0.1482	2171	0.7629	0.0115
0.2066	2130	0.7595	0.0113
0.2592	2116	0.7550	0.0109
0.3462	2073	0.7499	0.0104
0.3743	2055	0.7506	0.0103
0.3936	2051	0.7486	0.0101
0.4213	2057	0.7402	0.0098
0.4259	2102	0.7242	0.0093
0.4789	2105	0.7234	0.0089
0.5264	2103	0.7250	0.0085
0.6348	2063	0.7242	0.0076
0.7439	2043	0.7324	0.0067
0.8809	1987	0.7386	0.0063
0.9291	1968	0.7471	0.0082

The total dissolved air content of the oil was found to be a mass fraction of 0.000135 of the oil. In order for the compressible model to account for the two-phase flow effects observed in the tests, the gas bubble content would have to be as high as 0.02215 mass fraction. If the observed effects were due to the presence of a gaseous phase, the gaseous phase must have been primarily composed of hydrocarbon vapor. As suggested by Henry (6), a bubble formed in a liquid near saturation pressure would be composed almost entirely of vapor of the liquid. Thus it seems likely that much of the observed effects were due to cavitation of the oil, rather than being due to deaeration only. However, an indeterminate part of the observed effects could have been due to thermal expansion effects due to varying downstream oil temperature.

No theory is advanced concerning the reason for the increase in discharge coefficient at the transition from incompressible to compressible flow. This phenomenon was noticeable at the higher flow rates tested, and was quite repeatable at these flow rates. At the higher test flow rates it was possible to very precisely determine the transition pressure ratio, since the test apparatus could be adjusted so that the operating point would fluctuate from one side of the transition to the other. The sharply defined transition was not detected at the low flow rates. It is possible that the difference in discharge coefficient at transition was not as

great at the low flow rates, since the analysis of the data indicated compressibility effects were less at low flow rates. However, even if the difference in discharge coefficient at transition did occur at low flow rates, it would be extremely difficult to detect. At the lowest flow rate tested, the entire compressible flow regime was encountered within 0.0003 inch of valve travel. Thus it would be difficult to resolve more than three data points within the compressible flow regime at that flow rate, and it would be correspondingly difficult to resolve the transition point.

A literature search to determine the reason for the increase in discharge coefficient at transition to two-phase flow revealed counter examples. Wallis (19) indicated that the presence of a small amount of a gaseous phase in a liquid would increase fluid viscosity. Flow number, as reported herein, was calculated as a function of liquid viscosity, without consideration of the effects of the gaseous phase. Consequently, if the actual viscosity of the two-phase mixture was higher than assumed, the actual flow number would be lower. Discharge coefficient would be higher at this lower flow number, but to explain the observed difference in discharge coefficient at high flow number would require that viscosity would be greater by a factor of four, which seems improbable. Furthermore, if this were the case, much greater effects would be expected at low flow numbers where the slope

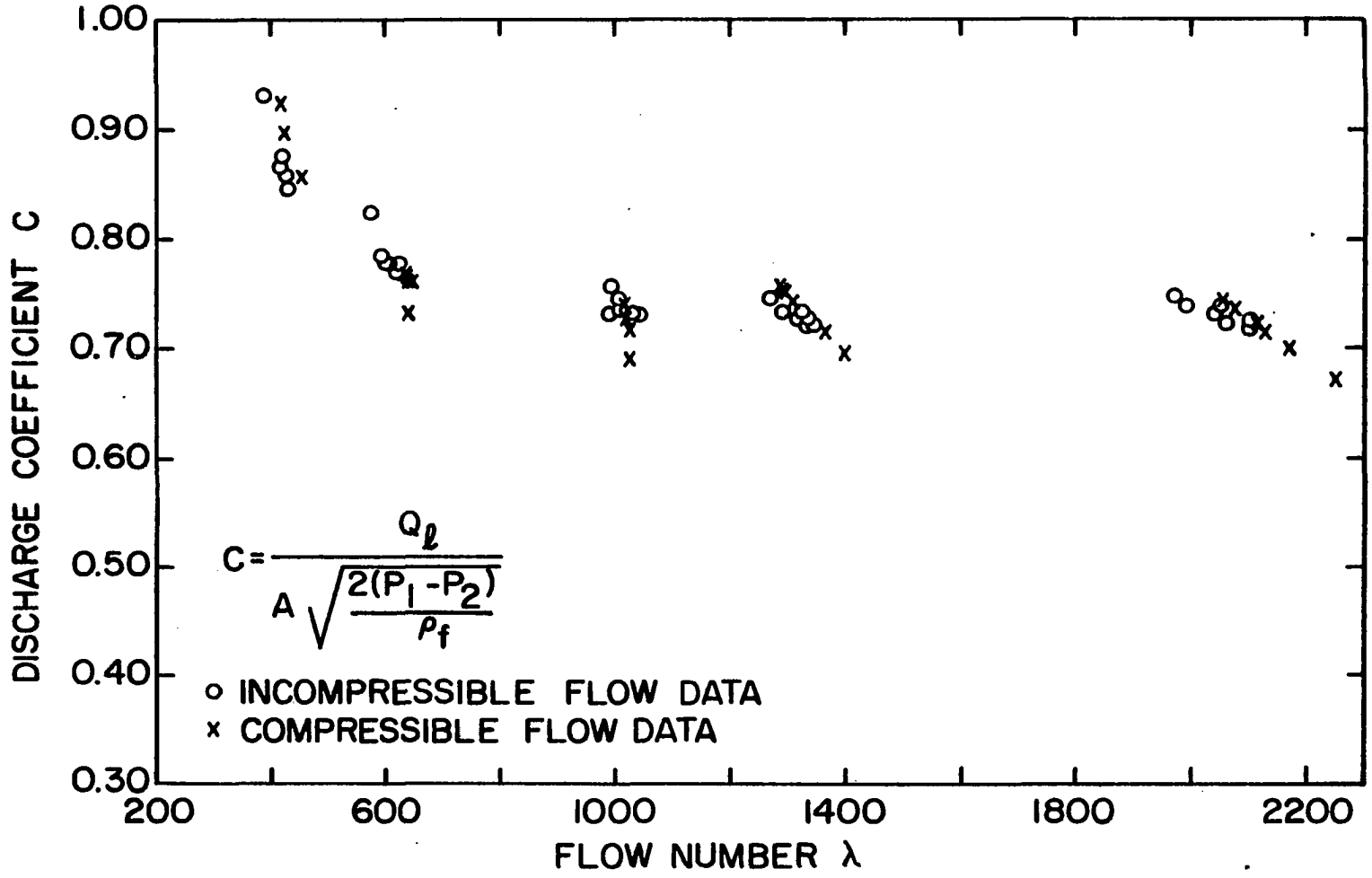

Figure 13. Discharge coefficient vs. flow number using incompressible model to analyze both compressible and incompressible flow data

of the curve in figure 9 is steeper. However, the difference in discharge coefficient at transition was not noticeable in the low flow number results.

It seems unlikely that the increase in discharge coefficient was due to an increase in pressure recovery, since previous research has shown that a gaseous phase tends to decrease pressure recovery in a fluid. Korstanje (10) established that the presence of a gaseous phase in a liquid would hinder pressure recovery in a diffuser. He theorized that this was due to two effects. The increased viscosity due to the presence of the gaseous phase increases boundary layer thickness, dissipating additional energy and thus hindering pressure recovery. However, he proposed that the major effect hindering pressure recovery was due to absorption of energy in compression of the gas phase.

Hench and Johnston (5) confirmed that the addition of a gaseous second phase decreased pressure recovery in a diffuser.

An attempt was made to utilize data collected by Storjohann to confirm the above results. His results did not correlate well with the results reported herein in that a rise in discharge coefficient was indicated at high pressure ratio regardless of flow number.

Several factors may be responsible for this apparent effect. When tested by Storjohann, the valve assembly was

clamped together using four 1/4 inch shafts threaded their entire lengths. The cross-sectional area of these fasteners was sufficiently low that when the pressure in the downstream cavity was high, the preload between the body blocks may have been lost, causing the body blocks to separate slightly. This would cause an incremental opening of the orifice that could not be detected with the valve position measuring micrometer, and the apparent discharge coefficient thus measured would be correspondingly high. The loss of preload would not be evidenced by leakage, since the joint was sealed by an "O" ring, which would retain the seal regardless of a few thousandths inch gap between the blocks.

In addition, the "O" ring gland dimensions were apparently not properly specified, and the volume of the "O" ring was as great as the volume of the gland cavity, or even possibly greater. If the volume of the "O" ring was greater than the volume of the gland cavity, a significant part of the preload would be borne by the less rigid "O" ring, resulting in a less rigid assembly. As downstream pressure would be increased, the joint would separate slightly, and this would again not be detected by the valve position measuring micrometer, but would be reflected as an increase in apparent discharge coefficient. It is a distinct possibility that a significant amount of the preload was borne by the "O" ring since, when the test valve was first disassembled by the

author, the "O" ring, which originally was toroidally shaped, had been remolded by the "O" ring gland into a nearly square section ring. The "O" ring gland was remachined to proper dimensions prior to the tests reported herein.

A relatively small part of the noted variation could have been due to thermal expansion effects, as described above.

CONCLUSIONS

1. Over the range of spool underlap positions tested, the effective orifice area of the one-half-inch diameter, 0.00029 inch radial clearance spool valve was satisfactorily described by the hyperbolic area function developed by Storjohann.
2. If the ratio of pressure downstream of the valve orifice to pressure upstream is sufficiently high, steady state flow through the spool valve is described by the incompressible flow hydraulic equation, with discharge coefficient decreasing as a function of flow number in the range of flow number tested.
3. If the ratio of pressure downstream of the valve orifice to pressure upstream is sufficiently low, steady state flow through the valve is not satisfactorily described by the incompressible flow hydraulic equation, but is more characteristic of compressible flow. The compressibility effect seems to be an approximately linear increasing function of flow number, and an approximately linear decreasing function of pressure ratio. It is assumed that this compressibility effect is due to the evolution of a gaseous phase from the liquid phase as it flows through the valve. Steady state, low pressure ratio flow is more adequately described by Kays' homogeneous flow model, if it is assumed that gas phase con-

tent is a linear increasing function of flow number, and a linear decreasing function of pressure ratio, even though Kays' model assumes that the gaseous phase is present in the fluid as the fluid enters the orifice, and that the pressure drop across the valve orifice was small compared to the downstream pressure.

RECOMMENDATIONS FOR FURTHER STUDY

It is suggested that the tests be repeated utilizing a different method of determining valve opening. A simple interchange of the valve positioning and valve position measuring micrometers on the present test valve would provide useful information concerning effects of thermal expansion. The upstream side of the test valve is continuously exposed to a steady stream of constant temperature fluid. The spool waist is immersed in this flow, and the rest of the upstream side of the spool is immersed in the radial clearance gap leakage flow, which is of consistent temperature distribution (although the leakage is throttled to atmospheric pressure as it passes through the clearance gap, it would have a consistent effect since the throttling effect would depend only on the upstream pressure, which is constant).

Some noticeable error might be caused by the varying quantity of heat conducted into the upstream side of the test valve body from the downstream side as test conditions vary. Since the upstream side of the spool would be quite constant in temperature, there would be no compensating expansion of the spool. Thus if any such error would be encountered, it would be opposite in sign from those encountered in the tests reported herein, and as such would at least be useful in confirming the source of error.

The upstream pressure acts on both interior surfaces of the spool ends, causing the spool waist to be extended axially. This is not seen to be a problem, since for a test with upstream pressure held constant, the amount of extension would be very nearly constant. The use of the ground plate to determine the micrometer reading corresponding to line-on-line spool position was found to be unsatisfactory due to the unpredictable thermal expansion of the spool, valve body, and micrometer. This method of calibration would be even more unsatisfactory if used to calibrate a micrometer on the upstream side of the valve since the thickness of the ground plate would have to be subtracted from the micrometer reading to determine valve line-on-line reading. This would introduce further possibilities of error, so it is felt that the valve line-on-line micrometer reading would have to be determined by least squares curve fit, as was done in the test reported herein. The fixed error due to axial expansion of the spool waist would not affect this procedure.

The valve could also be tested by allowing the valve to reach equilibrium with a uniform (and thus reproducible) temperature distribution, then rapidly shifting the operating point to test conditions and recording the data before significant thermal expansion effects would occur. The operating conditions could be shifted rapidly using solenoid operated valves. Valve position could be measured rapidly using

a linear variable displacement transducer. Pressures upstream and downstream of the orifice and valve position data could be recorded continuously by tape recording binary coded digital output from the API digital panel meters. This would allow nearly instantaneous reading of the data when flow conditions are shifted to the operating point, and also would facilitate study of the time response of thermal expansion effects.

The tests reported herein were conducted at the same temperature, and thus the same fluid viscosity. Flow number was varied by varying flow rate only. To confirm that discharge coefficient of the valve is the observed function of flow number, it would be desirable to repeat the tests at various temperatures, to vary flow number while maintaining flow rate constant. Such tests would also provide useful information concerning the effects of temperature on the deaeration and cavitation characteristics of the test fluid.

A method of measuring valve opening directly would be required in order to significantly improve the testing of the spool valve. McCloy and Beck (11) used direct visual observation of the opening of their test valve, with excellent results. However, the test valve used in the tests reported herein is not suitable for modification for visual observation of the opening, and the author has been unable to devise a non-visual method of directly measuring valve opening.

Henry (6) and others have used gamma ray attenuation systems to determine void fraction in two-phase flow study. Much valuable information concerning the two-phase aspects of spool valve flow could be gathered if such a device could be used to determine quality at the orifice of a two-dimensional simulated spool valve, such as reported by McCloy and Beck (11).

BIBLIOGRAPHY

1. Apkon, Nathan D. "An Instrument for the Continuous Measurement of Vapor/Liquid Ratio." 1969 Cavitation Forum. Edited by F. G. Hammitt and A. G. Grindel. New York, N.Y.: American Society of Mechanical Engineers, 1969.

2. Beers, Yardley. Introduction to the Theory of Error. Reading, Massachusetts: Addison-Wesley, 1957.

3. Epstein, P. S., and Plesset, M. S. "On the Stability of Gas Bubbles in Liquid-Gas Solutions." Journal of Chemical Physics, 18 (Nov., 1950), 1505-9.

4. Geiger, G. E. "Sudden Contraction Losses in Single- and Two-Phase Flow." Unpublished Ph.D. thesis, University of Pittsburgh, 1964.

5. Hench, J. E., and Johnston, J. P. "Two-Dimensional Diffuser Performance With Subsonic Two-Phase, Air-Water Flow." ASME 71-FE-20, 1971.

6. Henry, Robert E. "A Study of One- and Two-Component, Two-Phase Critical Flows at Low Qualities." Argonne National Laboratory ANL-7430, 1968.

7. Kays, W. M. "Loss Coefficients For Abrupt Changes in Flow Cross Section With Low Reynolds Number Flow in Single and Multiple Tube Systems." American Society of Mechanical Engineers Transactions, 72 (1950), 1067-74.

8. Kays, W. M., and London, A. L. Compact Heat Exchangers. Palo Alto, Calif.: National Press, 1964.

9. Khokhlov, V. A. "Hydraulic Loss and Fluid Discharge Coefficients Through the Orifices of a Cylindrical Spool-Valve Hydraulic Performance Mechanism." Avtomat. i. Telemekh., 16 (No. 1, 1955), 64-70. Original not available; cited in J. F. Blackburn. "Pressure-Flow Relationships for Hydraulic Valves." Fluid Power Control. Edited by John F. Blackburn; Gerhard Reethof; and J. Lowen Shearer. Cambridge, Massachusetts: The M.I.T. Press, 1960.

10. Korstanje, Hugo P. "The Pressure Recovery of a One-Component Two-Phase Flow in a Two-Dimensional Diffuser." Argonne National Laboratory ANL-7504, 1969.

11. McCloy, D., and Beck, A. "Some Cavitation Effects in Spool Valve Orifices." Proceedings of The Institution of

Mechanical Engineers Part I, London, 182 (No.8, 1967), 163-74.

12. MacLellan, G. D. S.; Mitchell, A. E.; and Turnbull, D. E. "Flow Characteristics of Piston-Type Control Valves." Proc. Symp. Recent Mech. Engr. Dev. in Auto. Control. 1960. Original not available; cited in D. McCloy and A. Beck. "Some Cavitation Effects in Spool Valve Orifices." Proceedings of The Institution of Mechanical Engineers Part I, London, 182 (No.8, 1967), 163-74.

13. Magorien, Vincent G. "Effects of Air on Hydraulic Systems." Hydraulics & Pneumatics, 20 (October, 1967), 128-31.

14. Magorien, Vincent G. "How Hydraulic Fluids Generate Air." Hydraulics & Pneumatics, 21 (June, 1968), 104-8.

15. Reethof, Gerhard. "Properties of Fluids." Fluid Power Control. Edited by John F. Blackburn; Gerhard Reethof; and J. Lowen Shearer. Cambridge, Massachusetts: The M.I.T. Press, 1960.

16. Shearer, J. L. "Dynamic Characteristics of Valve-Controlled Hydraulic Servomotors." American Society of Mechanical Engineers Transactions, 76 (1954), 895-903.

17. Storjohann, Donald R. "Flow and Fluid-Flow Force of Hydraulic Spool Valves." Unpublished Master of Engineering thesis, Iowa State University, 1972.

18. Tong, L. S. Boiling Heat Transfer and Two-Phase Flow. New York, N.Y.: John Wiley and Sons, Inc., 1965.

19. Wallis, Graham B. One-dimensional Two-phase Flow. New York, N.Y.: McGraw-Hill, 1969.

20. Zaloudek, F. R. "The Critical Flow of Hot Water Through Short Tubes." HW-77594, 1963. Original not available; cited in Robert E. Henry. "A Study of One- and Two-Component, Two-Phase Critical Flows at Low Qualities." Argonne National Laboratory ANL-7430, 1968.

ACKNOWLEDGMENTS

The author wishes to express his thanks to Professor Bruce L. Johnson for suggesting this study, and providing guidance and encouragement throughout the course of the study.

Additional gratitude is due Professor Johnson for serving as the author's co-major professor, along with Professor Morris H. Mericle. Thanks are also due to the other members of the author's graduate committee: Dr. Jerry L. Hall, Dr. Donald P. Young, and Dr. Robert J. Lambert.

The author would also like to acknowledge the assistance of the Iowa State University Department of Mechanical Engineering and the Iowa State University Engineering Research Institute, who have made this study possible.

APPENDIX A. CALIBRATED DATA

P_1	P_2	X	Q	T (^{o}F)
Flow Rate Number 1				
2019.8	48.2	0.00130	12.84	178.50
2019.8	556.1	0.00134	12.76	178.50
2019.8	694.2	0.00150	12.60	178.84
2019.8	926.2	0.00168	12.60	178.67
2019.8	1175.2	0.00195	12.60	178.67
2019.8	1457.4	0.00245	12.60	178.67
2019.8	1642.2	0.00305	12.60	178.67
2019.8	1817.2	0.00405	12.53	178.67
2019.8	1928.2	0.00565	12.60	178.67
Flow Rate Number 2				
2019.8	53.2	0.00195	16.11	178.50
2019.8	278.2	0.00205	16.58	178.50
2019.8	415.2	0.00215	16.74	178.50
2019.8	566.2	0.00225	16.66	178.50
2019.8	685.2	0.00235	16.74	178.83
2019.8	794.0	0.00245	16.74	178.83
2019.8	986.2	0.00265	16.58	178.83
2019.8	1184.2	0.00295	16.74	178.83
2019.8	1385.1	0.00335	16.50	178.83
2019.8	1563.2	0.00395	16.50	178.83
2019.8	1731.2	0.00495	16.50	178.83
2019.8	1883.6	0.00695	16.74	178.83
Flow Rate Number 3				
2019.8	69.2	0.00315	24.18	178.83
2019.8	301.2	0.00335	25.05	178.83
2019.8	493.2	0.00355	25.37	178.83
2019.8	660.2	0.00375	25.77	178.83
2019.8	792.1	0.00395	25.61	178.50
2019.8	966.2	0.00425	25.29	178.83
2019.8	1272.2	0.00515	25.84	179.16
2019.8	1429.2	0.00575	25.61	179.16
2019.8	1613.2	0.00695	25.69	178.83
2019.8	1767.2	0.00875	25.92	179.16
2019.8	1904.0	0.01275	26.00	179.16

P_1	P_2	X	Q	T (^{O}F)
Flow Rate Number 4				
2019.8	168.2	0.00425	32.01	178.00
2019.8	340.2	0.00435	32.01	178.00
2019.8	508.2	0.00445	31.93	178.00
2019.8	599.2	0.00455	32.01	178.00
2019.8	703.2	0.00465	32.01	178.00
2019.8	753.0	0.00475	32.01	178.00
2019.8	805.6	0.00485	31.93	178.00
2019.8	878.2	0.00515	32.01	178.00
2019.8	1063.2	0.00565	31.93	178.00
2019.8	1205.2	0.00615	31.93	178.00
2019.8	1318.2	0.00665	31.93	178.00
2019.8	1608.1	0.00865	31.93	178.00
2019.8	1772.2	0.01105	31.93	178.00
2019.8	1900.0	0.01565	32.01	178.00
Flow Rate Number 5				
2039.9	137.2	0.00655	48.21	178.70
2019.8	299.2	0.00665	48.52	178.70
2019.8	417.2	0.00676	48.44	178.70
2019.8	523.4	0.00695	48.68	178.70
2019.8	699.2	0.00725	48.60	178.70
2019.8	756.1	0.00735	48.60	178.70
2019.8	795.0	0.00745	48.60	178.70
2019.8	851.0	0.00765	48.52	178.70
2019.8	860.2	0.00785	48.52	178.70
2019.8	967.2	0.00825	48.52	178.70
2019.8	1063.2	0.00865	48.60	178.70
2019.8	1282.2	0.00985	48.52	178.70
2019.8	1502.5	0.01165	48.60	178.70
2019.8	1779.2	0.01695	48.60	178.70
2019.8	1876.5	0.02175	48.68	178.70

APPENDIX B. REDUCED DATA

P_2/P_1		C (Compressible Model)	C (Incompressible Model)	C (Mathematical Model)	x Quality	K
Flow Rate Number 1						
0.0239	451	0.8851	0.8579	0.8427	0.00498	0.024
0.2753	415	0.9306	0.9232	0.8792	0.00168	0.380
0.3437	420	0.9012	0.8976	0.8732	0.00091	0.524
0.4586	426	0.8871	0.8871	0.8661	0.00000	0.847
0.5819	421	0.8748	0.8748	0.8713	0.00000	1.392
0.7216	427	0.8584	0.8584	0.8648	0.00000	2.591
0.8131	430	0.8448	0.8448	0.8617	0.00000	4.350
0.8997	414	0.8658	0.8658	0.8804	0.00000	8.973
0.9547	387	0.9308	0.9308	0.9232	0.00000	21.067
Flow Rate Number 2						
0.0264	640	0.7650	0.7325	0.7721	0.00702	0.027
0.1378	641	0.7846	0.7635	0.7720	0.00505	0.160
0.2056	640	0.7817	0.7667	0.7721	0.00384	0.259
0.2803	632	0.7760	0.7671	0.7734	0.00248	0.390
0.3393	632	0.7758	0.7709	0.7736	0.00144	0.513
0.3931	627	0.7739	0.7723	0.7744	0.00049	0.648
0.4883	618	0.7714	0.7714	0.7761	0.00000	0.954
0.5863	622	0.7793	0.7793	0.7753	0.00000	1.417
0.6858	608	0.7775	0.7775	0.7781	0.00000	2.182
0.7739	600	0.7789	0.7789	0.7798	0.00000	3.424
0.8571	596	0.7830	0.7830	0.7807	0.00000	6.000
0.9326	573	0.8247	0.8247	0.7863	0.00000	13.836
Flow Rate Number 3						
0.0343	1024	0.7374	0.6905	0.7409	0.01101	0.035
0.1491	1025	0.7471	0.7172	0.7408	0.00775	0.175
0.2442	1018	0.7454	0.7277	0.7411	0.00501	0.323
0.3269	1014	0.7506	0.7417	0.7413	0.00266	0.486
0.3922	1009	0.7369	0.7369	0.7414	0.00000	0.645
0.4784	990	0.7307	0.7307	0.7422	0.00000	0.917
0.6299	1043	0.7320	0.7320	0.7401	0.00000	1.702
0.7080	1034	0.7316	0.7316	0.7405	0.00000	2.424
0.7987	1031	0.7319	0.7319	0.7406	0.00000	3.968
0.8750	1007	0.7449	0.7449	0.7415	0.00000	6.998
0.9427	993	0.7578	0.7578	0.7421	0.00000	16.452

P_2/P_1		C (Compressible Model)	C (Incompressible Model)	C (Mathematical Model)	x Quality	κ
Flow Rate Number 4						
0.0833	1398	0.7499	0.6970	0.7312	0.01314	0.091
0.1685	1363	0.7511	0.7151	0.7319	0.00958	0.203
0.2516	1322	0.7573	0.7352	0.7326	0.00624	0.336
0.2967	1310	0.7592	0.7436	0.7329	0.00454	0.422
0.3482	1289	0.7646	0.7559	0.7333	0.00262	0.534
0.3728	1291	0.7602	0.7545	0.7333	0.00174	0.594
0.3989	1290	0.7556	0.7530	0.7333	0.00081	0.663
0.4348	1327	0.7334	0.7334	0.7325	0.00000	0.769
0.5264	1332	0.7288	0.7288	0.7325	0.00000	1.112
0.5967	1337	0.7258	0.7258	0.7324	0.00000	1.480
0.6527	1341	0.7234	0.7234	0.7323	0.00000	1.879
0.7962	1315	0.7266	0.7266	0.7328	0.00000	3.907
0.8774	1289	0.7339	0.7339	0.7333	0.00000	7.160
0.9407	1264	0.7469	0.7469	0.7339	0.00000	15.858
Flow Rate Number 5						
0.0673	2249	0.7580	0.6729	0.7229	0.02213	0.072
0.1482	2171	0.7629	0.7016	0.7234	0.01648	0.174
0.2066	2130	0.7595	0.7140	0.7237	0.01271	0.260
0.2592	2116	0.7550	0.7222	0.7237	0.00954	0.350
0.3462	2073	0.7499	0.7359	0.7240	0.00433	0.530
0.3743	2055	0.7506	0.7420	0.7241	0.00269	0.598
0.3936	2051	0.7486	0.7436	0.7242	0.00158	0.649
0.4213	2057	0.7402	0.7402	0.7241	0.00000	0.728
0.4259	2102	0.7242	0.7242	0.7238	0.00000	0.742
0.4789	2105	0.7234	0.7234	0.7238	0.00000	0.919
0.5264	2103	0.7250	0.7250	0.7238	0.00000	1.112
0.6348	2063	0.7242	0.7242	0.7241	0.00000	1.739
0.7439	2043	0.7324	0.7324	0.7242	0.00000	2.904
0.8809	1987	0.7386	0.7386	0.7246	0.00000	7.397
0.9291	1968	0.7471	0.7471	0.7248	0.00000	13.096